ENME 304 Machine Design
Final Design Update

Submitted to Professor Janelle Clark
12/17/25

Group 10 Members-
Adam Beall
Bilal Faizullah
Ian Wright
John Xavier

1. Executive summary

The ENME 304 Lift Platform Challenge required the design, analysis, fabrication, and demonstration of a mechanically driven device capable of lifting a specified payload to a target height whilst satisfying dimensional, power, safety, and budgetary constraints. The objective of this project was to apply machine design principles such as drivetrain design, load transmission, material selection, and failure analysis, to produce a compact and efficient lifting mechanism.

The final design was a scissor lift mechanism driven by a custom gear and pulley drivetrain powered by the provided Mabuchi RS-555PH-3255 DC motor and 12 V battery. The system was designed to be self-standing within an 8x8x8 inch volume at the beginning of operation and raise its lifting platform to a minimal height of 12 inches without the usage of stored mechanical energy. Analytical modeling was performed on all major machine elements such as the shafts, gears, fasteners, and structural members to ensure the stress, deflection, and fatigue criteria were within compliance.

The fabrication process included a combination of fully machined components and rapid prototyping. Load-bearing elements such as the scissor lift arms and the structural L-brackets were machined to ensure proper alignment and dimensional consistency. Rapid prototyping through 3D printing was used extensively in the creation of the drivetrain. A complete CAD model was developed and maintained throughout the design process for the sake of having a reference model and ease of 3D printing.

During the final assembly prior to demonstration, a localized failure occurred in the final output shaft connecting the drivetrain to the pulley, which was our lifting mechanism. This prevented us from being able to use our machine at the demonstration. This failure was not due to a system-level error in the drivetrain or design, but rather due to the material and manufacturing error. Despite this, the overall design met the project requirements and the failure provided insight towards material selection and tolerance considerations.

Overall, the project successfully demonstrated the application of mechanical design principles, collaborative engineering, and problem solving under real-world constraints.

2. Introduction/Project Background

The ENME 304 Lift Platform Challenge required the design, analysis, fabrication, and demonstration of a mechanically driven device that is capable of lifting a specified payload to a target height under dimensional and power constraints. The purpose of this project was to emphasize the practical application of machine design principles including drivetrain design, load transmission, component sizing, and failure analysis, whilst also accounting for manufacturability and the cost.

The device was required to fit within a cube with an 8x8x8 inch volume at the start. It would need to lift a payload of at least 3.1lb, preferably 5lb, to a height of 12 inches with a single DC motor and battery as the power source. These constraints played a significant role in the creation of our drivetrain. The system was also to be self-standing, operate without stored mechanical energy, and complete lifting and resetting operations under timed conditions, further influencing our decisions related to gear ratios and structural layout.

The final design focused on a scissor lift mechanism driven by a gear train and pulley based system to maximize lift height, maintain compliance with all constraints, and of course reduce the complexity of the system. Throughout the project with analytical modeling and refinement, we ensured that the machine's components satisfied strength, deflection, and fatigue requirements.

During initial stages of the project, we encountered challenges in accurately determining the gear ratio and corresponding torque required for the lift, leading to issues in our first few design updates. The delayed feedback from experts regarding those led to our corrections not being able to be fully fulfilled. As a result, certain calculations were completed without accounting for certain factors, e.g. the shear and moment diagrams and it being completed without bearings.

3. Teams Design Process, Goals, and Strategies

3.1 - Design Conception and Problem Solving

The design process for this project followed a structured engineering approach that went from concept generation to detailed analysis, fabrication, and testing. The primary goal was to design a lifting mechanism that could lift a 3.1-5.0 lb load to a height of at least 12 inches whilst in a 8 by 8 by 8 inch cube under strict power, time, and budget constraints.

During the early stages of the project, several assumptions were made to allow for a rapid generation and comparison of initial design concepts, such as ideal power transmissions with no friction loss and uniform load distributions. Three primary concepts were initially generated: a screw lift, a rack and pinion lift, and a scissor lift. Each was evaluated on their feasibility with the constraints we were put under, leading to the screw lift's elimination due to excessive gear reduction requirements and the rack lifts complexity, dimensional issues, and slew speed. The

scissor lift was designed due to its best fit for the constraints and the greatest vertical lifting height. Throughout the design process itself however, we faced many challenges such as torque limitations, manufacturability, drivetrain layout, material selection, budget constraints, and assembly-related fitment issues. In particular, limitations associated with the available shaft stock within our budget and rapid-prototyped components influenced several iterations of our design and the required adjustments during fabrication. These challenges would lead to our final design of a simple and compact system.

3.2 - Team Collaboration and Contribution

The project was executed as a collaborative effort with responsibilities distributed among team members according to the project's Gantt Chart. Task ownership was assigned to ensure accountability whilst still allowing teamwork, overlap, and reviewing.

Adam Beall led the early conceptual and analytical phases of the project with his primary responsibilities being leading the brainstorming sessions, reviewing project rules and specifications, evaluating alternative design concepts, and preparing the Preliminary Design Review (PDR). Adam also led the final design calculations related to the drivetrain performance and load requirements, contributed to prototyping effort, and played a key role in drafting the initial version of the final report and preparing the final demonstration.

Bilal Faizullah was responsible for project planning and materials management. He created and continuously updated the project Gantt chart, ensuring alignment with milestones and keeping the team on track. Bilal led the submission of the updated design, initiated and completed the Bill of Materials (BOM), managed all of the material ordering, and coordinated trial runs prior to the final demonstration.

Ian Wright focused on concept development and design evolution. His contributions included the revising and narrowing of initial concepts, elaborating on realistic mechanisms, developing early prototype concepts, and refining the final design description. Ian led both the PDR presentation and the project's demonstration and disassembly.

John Xavier was primarily responsible for CAD modeling and supplier research. He identified potential suppliers early in the project and created both the prototype and final CAD models. He incorporated feedback from the PDR and verified compliance with project requirements. John also contributed to the final report completion and ensured that the final design met all dimensional and functional constraints

This division of responsibilities ensured a balance of contributions across conceptual design, analysis, creation, procurement, and documentation whilst maintaining continuous collaboration throughout the semester.

3.3 - Gantt Chart

The project schedule and task allocation were managed via a Gantt chart developed early into the project and continuously updated as required. The chart documents all major phases, milestones, and individual responsibilities for each team member. The final Gantt chart, including task ownership and completion timelines, is included in Appendix A as required.

3.4 - Group Brainstorming, Evaluation, and Problem Solving Reporting

3.4.1 - Initial Concepts and Ideas

When we were initially given our design criteria we decided to do a brain storming session and came up with 3 concepts to achieve the designated goal. The first was a screw lift suggested by John Xavier, this is a system that utilizes a central threaded shaft and a powered nut. It works by rotating the nut around the shaft which rotates whatever is attached to the nut up the shaft obtaining vertical height. Our second design idea was a scissor lift proposed by Adam Beall, this idea utilizes 2 pairs of crossed beams to support a platform. This design is powered by having one end of the crossed beams pinned and the other free floating on or in a track. This causes the crossed beams to dynamically move around a shared pivot increasing the height of the system. Our third and final idea was a rack lift also proposed by John Xavier, This involved using a set of spur gear on a racked gear system supporting the corners of a platform. When in motion the gears would climb vertically up the gear racks and push the platform up. During about a week of deliberation we came to settle on the scissor lift as our final design. This was because the other 2 ensign ideas just had too many shortcomings to overcome when compared to the scissor lift. For the screw lift the most critical shortcoming that doomed this idea was the speed of the system. The screw lift was a very efficient system by being able to move larger loads than other systems per the same input of energy but it just does not have the speed to work within our constraints because by the time the required height is reached the allotted time frame would be long overdue. In our deliberations the rack lift idea was also discarded because when we evaluated the hardware required to create the system it was deemed way too expensive for us to design a reliable system in the allotted budget.

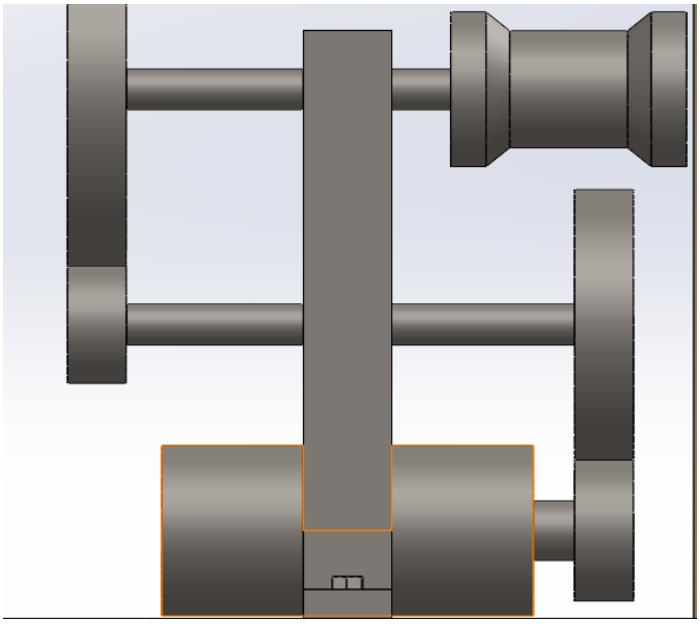

Figure 1 : Photo of Initial CAD Design for Gear Train

3.4.2 - Final Design Decision

With us deciding on a scissor lift design we had to make some initial considerations that would affect the whole framework of our design. This was the decision to use a single scissor lift section rather than multiple to achieve the desired height. We realised that if we carefully designed a single scissor lift section it would be able to make the 4 inch height change without much difficulty, allowing for us to tweak our design to increase the height by 5 inches instead. In order to reach the total height of 12 inches however, it was going to need a boost. This came in the shape of a frame we built to hold the scissor lift up higher in the air so it could start as close to the 8 inch starting height as possible (Figure 1). This was very advantageous because not only would we have an allowable margin of error in our design if something wasn't dimensionally accurate but it would also give us a perfect place for our power plant. This solved a major issue because the power plant consisting of the electric motor, gear train, battery, and electrical wiring/switch take up a large volume so this empty space below the scissor lift mechanism is perfect.

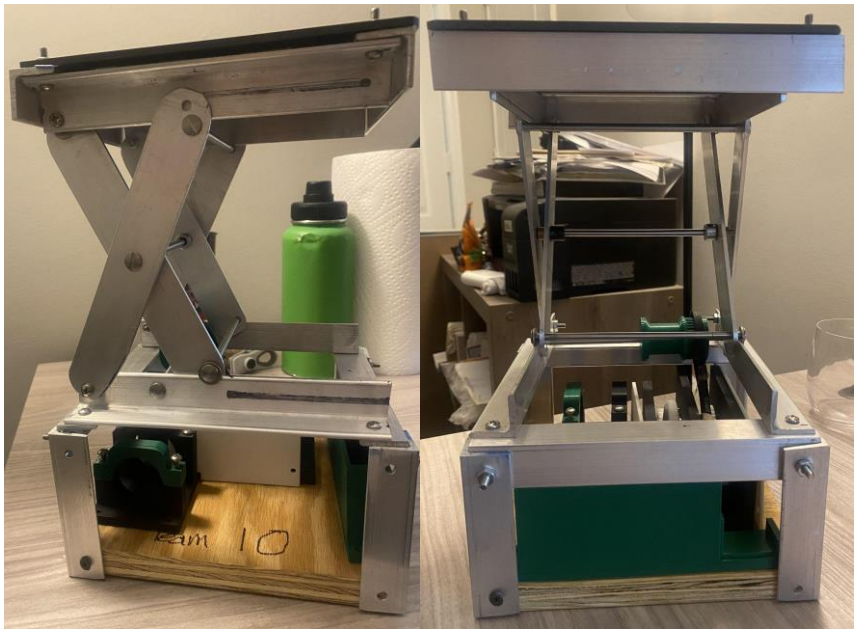

Figure 2 : Photo of Scissor Lift Mechanism

3.4.3 - Final Power Amplification and Delivery Decisions

In our initial designs we initially wanted to create a vertical gear train that would build up into the inside of our gear train to allow for the scissor lift to be retracted from a level plane allowing efficient transmission of power. This turned out to be an incorrect decision because we needed to have our gear train shafts fixed on both ends which required us to do a redesign. This quite significantly changed how our power plant was going to be structured, turning it into a flat gear train with a pinion gear powering 3 shared shafts with 2 gears each (Figure 5). This allowed us to translate power horizontally to a pulley we had linked up to the final drive shaft. This pulley is where we used a belt to translate the power vertically up to a spool, which would then retract our scissor lift and put it into motion.

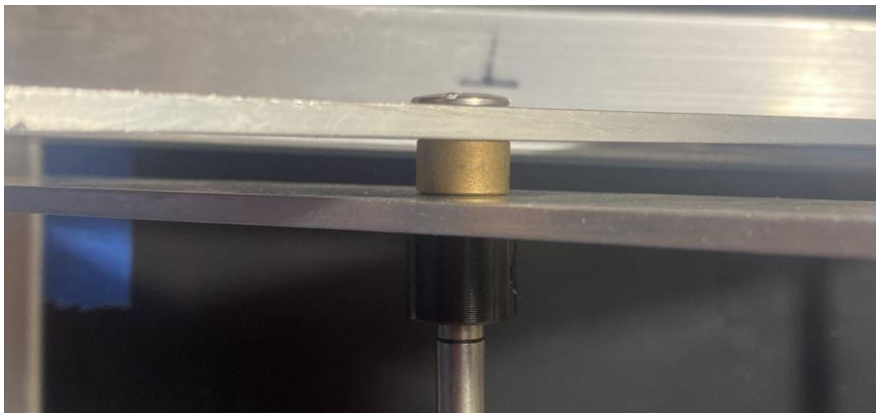

Figure 3 : Photo of Shaft Collar keeping Scissor Lift Arms in place

3.4.4 - Finalization Of Prototype Design

Our final design pulled in everything from our design and power/delivery decision together (Figure 7). This didn't do anything new or revolutionary but let us do some final tweaks to the system so everything was running smoothly. For example this allowed us to solve the problem of belt tensioning which was a challenge because we were not allowed to use springs in any context so belt tensioners were out of the question. We solved this problem however by mounting the gear train in a specific spot to our mounting plate so the distance the belt has to travel would put the belt into tension thus tensioning the belt.

Figure 4 : Photo of Battery and Switch Mount

3.5 - Design Testing, Prototyping, and Evolution

Prior to the demonstration, we were able to test our motor, belt fitment, scissor lift (Figure 2) under dynamic motion, battery and switch mount (Figure 4), and our soldered circuit with fuse. The first thing we were able to test was if the motor and circuit worked well together. We discovered that it worked perfectly with us being able to run the motor in both the clockwise and counter clockwise directions. This was further amplified by us not managing to blow out any of our 2 Amp fuses, meaning we were not overworking our system. Next we were able to test the scissor lift's mechanism (Figure 2) with our initial test showing us that the scissor lift was unexpectedly unstable because the scissor lift arms were having trouble staying captive at each end of the platform.

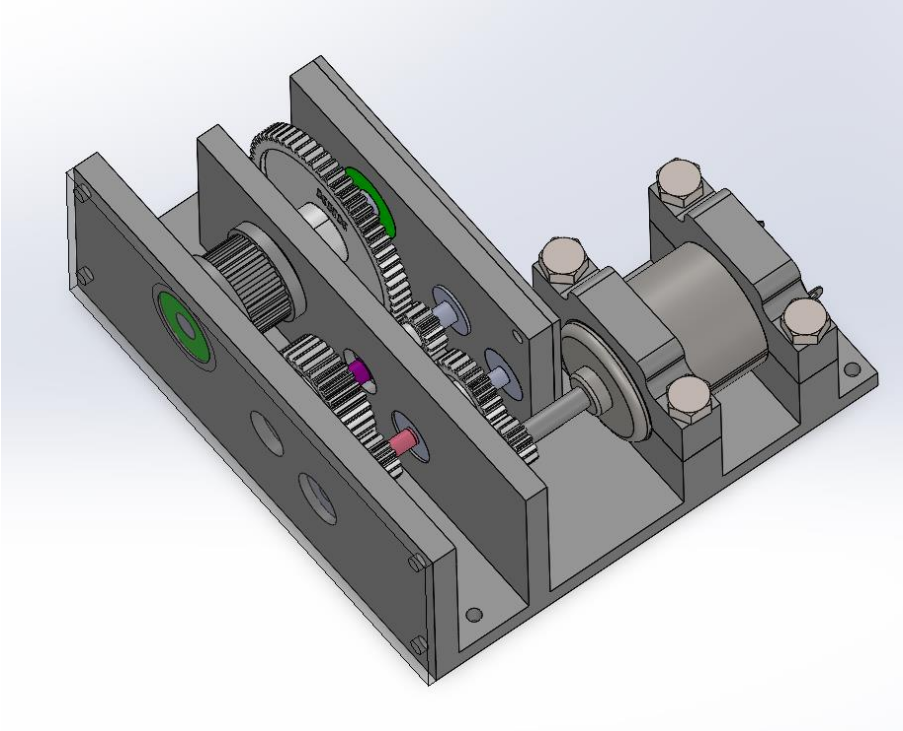

Figure 5 : Photo of Final Cad Design Gear for Train

To solve this we needed to add some shaft collars to our central shafts to keep them captive at either end of the scissor lift so the system can stay rigid and stable (Figure 3). For our belt we were initially thinking of using a multipart belt that could be pieced together and thus have its length change. This would have allowed us to tension the belt without requiring us to position the gear train in a specific place. This did not end up working because while the belt was made of multiple parts this came with the side effect of us losing surface area that is in contact with the pulley so we did not have the confidence that the belt wouldn't slip. This led us back to a more traditional belt with teeth on the inside, so after measuring the belts dimensions we were able to print a specially fit pulley for our belt. This eliminated the worries we had regarding the slip and thus loss of power because of it so this was a critical point of failure we had to address urgently.

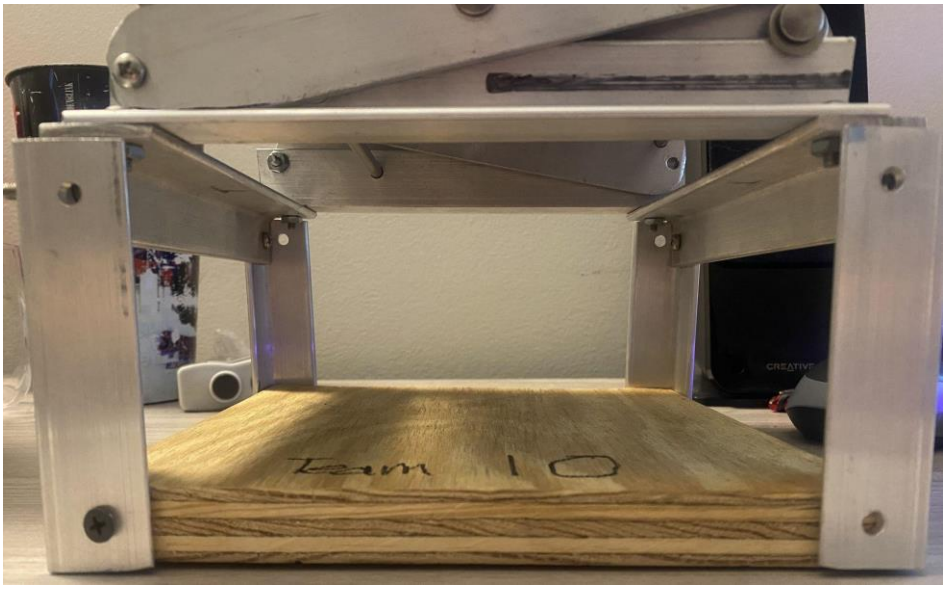

Figure 6 : Photo of Scissor Lift With Frame and Space for Power Plant Systems

(a) Extended Lift

(b) Compressed Lift

Figure 7 : Photo of Fully Assembled Scissor Lift Design

4. Design Model/Analysis

4.1 - Power Plant Design Decisions and Calculations

4.1.1 -Pulley's Design and Specifications

Pulley #1 (Figure 8) - 3D Printed Lower Pulley designed to key into our transmissions shaft so we could transmit power from our transmission vertically up to the 2nd Pulley driving the spool

Diameter - 0.55 inches Number of Timing Teeth - 28

Pulley #2 (Figure 8) - 3D Printed Upper Pulley designed with a spool which served as the powered pulling mechanism for our scissor lift.

Diameter - 0.65 inches Number of Timing Teeth - 37

(a) Pulley Attached to Gear Train

(b)Pulley Attached to Lift

Figure 8 : Left Pulley #1 and Right Pulley #2

4.1.2 - Belt Specifications

We decided to go with a timing belt because this belt seemed to perfectly solve our power transmission issue that required us to translate the power vertically by several inches. With only a relatively small load to bear and our confidence we could create a pulley to accommodate the belt this belt was an excellent choice so we did not have to work about slip being the major weak point of most belt designs.

Material - Neoprene Fiber glass reinforced Torque to withstand - τ = 8.07 lbf-in

Number of Teeth - 150 Pitch - 0.08 inches Tooth Type - Tapezoidal

Elastic Modulus- E = 870.226 Psi Belt Weight - w = 8.819*10^-3

Rotational Speed - ω = 3950 RPM $= 3950 * (\frac{2\pi}{60}) = 413.643$ Rad/sec

Belt thickness t = .08 in Belt Area - $A = b * t = .25 * .08 = .02\ in^2$

Outer Belt Length - 12 inches Width - b = ¼ inch

4.2.3 - Belt Force Analysis and Calculations

In order to ensure our selected timing belt would be sufficient, we calculated the tension that is applied to our belt under load and dynamic operation.

First we needed to calculate the required distance between our two pulleys (Figure 9)

$$C_{P1} = \frac{1}{2}(\pi r) = \pi r = .8639\ in$$

$$C_{P2} = \frac{1}{2}(\pi r) = \pi r = 1.0210\ in$$

$$2C = L - C_{P1} - C_{P2} = 10.115\ in$$

$$C = 5.0575\ in$$

Next we wanted to find the belt's angles of attachment to ensure we had enough surface area. (Figure 9)

$$\phi_{P1} = \pi - Sin^{-1}(\frac{D-d}{2}) = 3.122\ Rad$$

$$\phi_{P2} = \pi + Sin^{-1}(\frac{D-d}{2}) = 3.161\ Rad$$

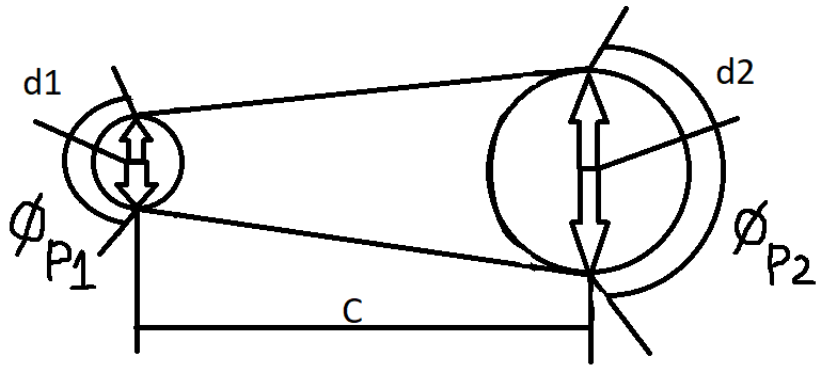

Figure 9 : Pulley FBD

Finally we need to calculate all forces affecting the belt which includes the centrifugal force during operation, the tensile force from belt tensioning, and the tension applied to each side of our pulleys from the torque.

$$F_C = \frac{w}{g}(\frac{V}{60})^2 = 9.85 * 10^{-4} lbf$$

$$E = \frac{FL}{A\Delta L} \rightarrow F_T = \frac{EA\Delta L}{L} = 17.637\ lbf$$

Tension on each end of 1st Pulley (Figure 10)

$$\tau = (F_1 - F_2)r_1 \rightarrow (F_1 - F_2) = \frac{\tau}{r_1} \rightarrow (F_1 - F_2) = 29.346\ lbf - in$$

$$F_1 = F_T + F_c + (\frac{F_1 - F_2}{2}) = 32.223\ lbf$$

$$F_2 = F_T + F_c - (\frac{F_1 - F_2}{2}) = 2.877\ lbf$$

Tension on each end of 2nd Pulley (Figure 11)

$$\tau = (F_1 - F_2)r_2 \rightarrow (F_1 - F_2) = \frac{\tau}{r_2} \rightarrow (F_1 - F_2) = 24.831\ lbf - in$$

$$F_1 = F_T + F_c + (\frac{F_1 - F_2}{2}) = 30.054\ lbf$$

$$F_2 = F_T + F_c - (\frac{F_1 - F_2}{2}) = 5.223\ lbf$$

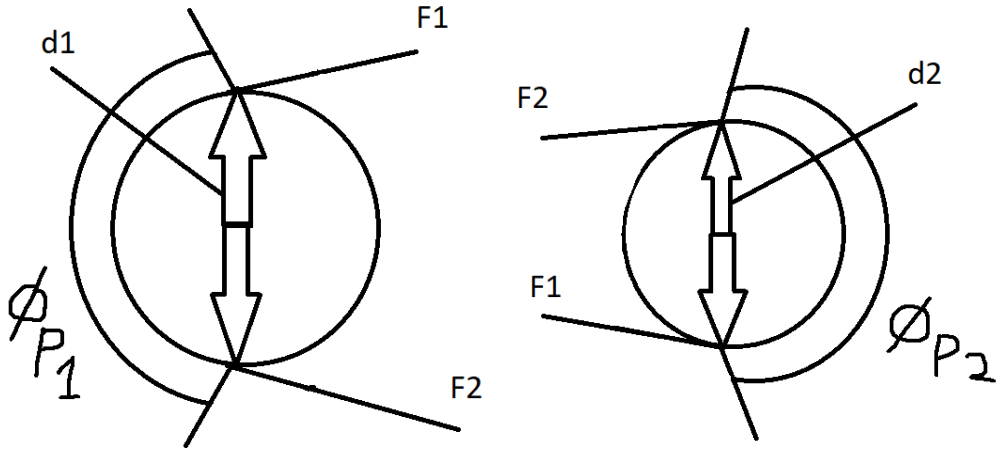

Figure 10 & 11 : Force FBD Analysis of each Pulley, Left Figure Pulley 1, Right Figure Pulley 2

With the forces on our belt calculated we can now compare it to our data. Since our manufacturer did not provide strength recommendations we found a Force analysis spread sheet

done on the same type of belts to give us an estimate[8]. This gave us a maximum strength of 51 lbf which, when compared to our belts, means we are at least 18 lbf less than our maximum. This would give us good confidence our belt would withstand the load.

4.1.4 - Gear Train Design, Forces, and Performance

When calculating for our Gear train, we first looked at the total weight we needed to lift which would include 3lbs and the plate which weighed 1.753lbs, adding these together, our total weight would be 4.753lbs. To find the torque required we would need to multiply the total weight by the distance which would be 4 in.

$$T_{req} = Total\ Weight * Distance = 19.012\text{lbf-in}$$

We then multiplied our factor of safety for our design which would be 1.5 to eliminate some errors.

$$T_{calc} = T_{req} * FOS = 28.518\text{lbf-in}$$

We also converted the input torque which would be taking the motors rated torque of .33lb-in and multiplying by the ratio of the current going through the motor (2.45A)over the max current we are allowing (2A). This would give our total torque input to be .269lbf-in for the motor limited to 2A. We then found our gear ratio with the input torque over our output.

$$Gear\ Ratio = \frac{T_{in}}{T_{calc}} = \frac{1}{106.014}$$

From our gear ratio being 1:106.014 which can be rounded to 110:1 for easy calculations. Since our gear ratio is greater than 100, we split our gear train into 3 stages. We calculated our smallest number of teeth without interference, assuming k being 1, m being our gear ratio of 110, and our pressure angle being 25°.

$$N_p = \frac{2k}{(1+2m)sin^2\phi}(m^2 + \sqrt{m^2 + (1+2m)sin^2\phi} = 11.15 \rightarrow 12 \text{ teeth}$$

With our smallest number of teeth being 12, we made our pinion gear connected to the motor. We can then find our gear train values through finding easy factors of 110 where,

$$\frac{N_3}{N_2} = 2, \frac{N_5}{N_4} = 5, \text{ and } \frac{N_7}{N_6} = 11$$

We also assumed that $N_2 = N_4 = N_6 =$ our minimum teeth number of 12 which gives,

$$N_3 = 24, N_5 = 60, \text{ and } N_7 = 132.$$

In the beginning of the semester, we miscalculated our torque to be 8 lbf-in. This error resulted in incorrect gear ratios and gear teeth calculations different than the corrected ones above. The gear teeth we purchased based on previous calculations are listed below.

$$N_1 = N_3 = N_5 = 12$$

$$N_2 = 24$$

$$N_4 = 36$$

$$N_6 = 60$$

Due to these gears being the ones that were purchased, the calculations throughout the rest of the report are based off of the gears purchased, not the corrected gear calculations.

4.2 - Statistical Analysis of assembled components

4.2.1 - Statistical Analysis and FBD's

When calculating the reaction forces on the plate, we did a super position of one arm taking into account the 5lb weight and another taking into account the weight of the plate. Shown in figures 12 and 13. When calculating for figure 12 we used table A9, 10 [5] where $l = Overall\ length = 7.55in$, $a = 3.82in$, and $b = 3.73in$. When then found ${F_{y1}}' = \frac{fb}{l} = 2.47lbf$, $f_x = 0$, and ${f_{y2}}' = \frac{fa}{l} = 2.53lbf$. For figure 13 we used table A9,7 where $w = .286in$ and $l = 3.82in$. Where ${F_{y1}}" = {F_{y2}}" = \frac{wl}{2} = .546\ lbf$. When combining the two superpositions, the reaction forces on the plate $F_{y1} = {F_{y1}}' + {F_{y1}}" = 3.016lbf$ and $F_{y2} = {F_{y2}}' + {F_{y2}}" = 3.076lbf$.

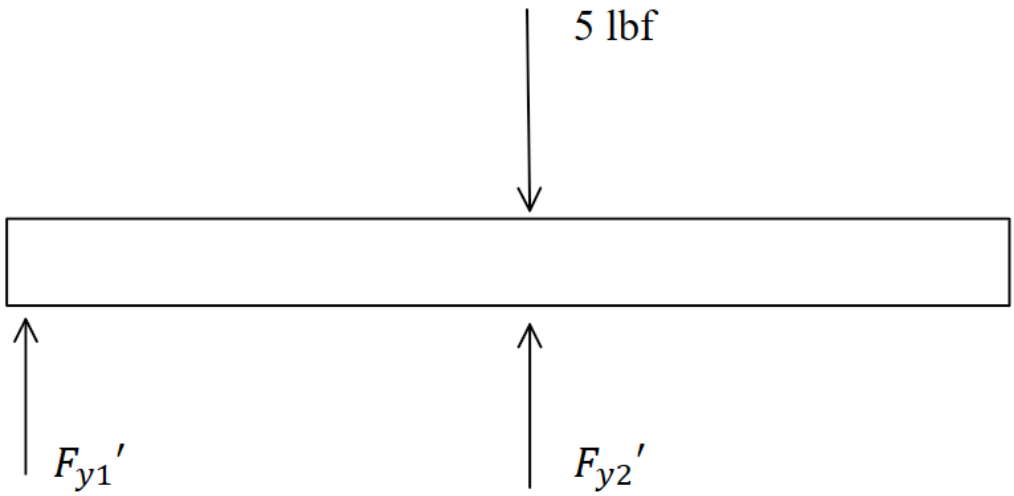

Figure 12 (Superposition 2): point load

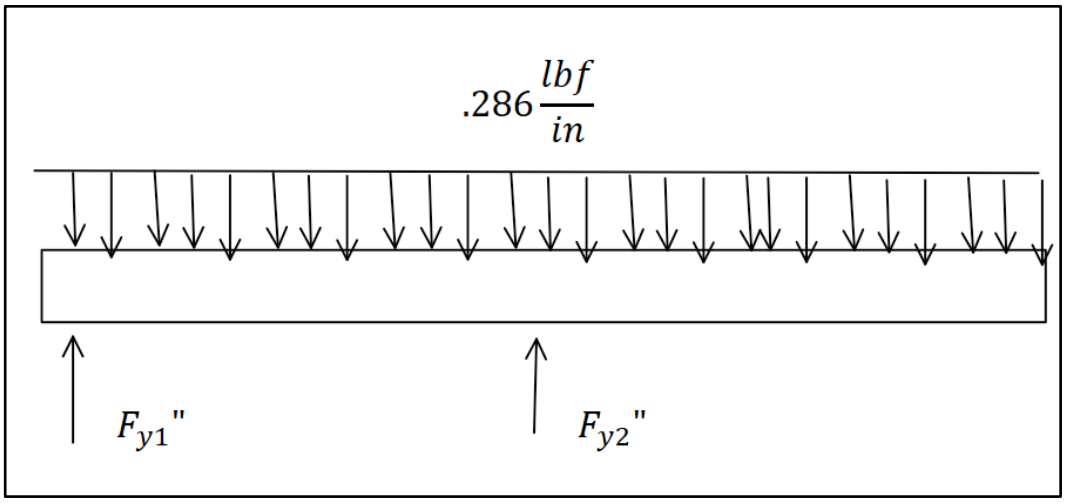

Figure 13 (Superposition 1): Superposition of the top plate uniform load

We then calculated the scissor lift arms shown in figure 14 and 15. Where $\theta = cos^{-1}(\frac{a}{l}) = 56.93^{o}$ in Figure 14. When finding our forces on the pins combining the two, $P_x = R_{x2} = \frac{F_{y2}+F_{y1}}{tan\theta} = 3.97lbf$, $P_y = F_{y1} - F_{y2} = -.06lbf$, $R_{y1} = F_{y1} - P_y = 3.076lbf$, and $R_{y2} = F_{y2} + P_y = 3.016lbf$.

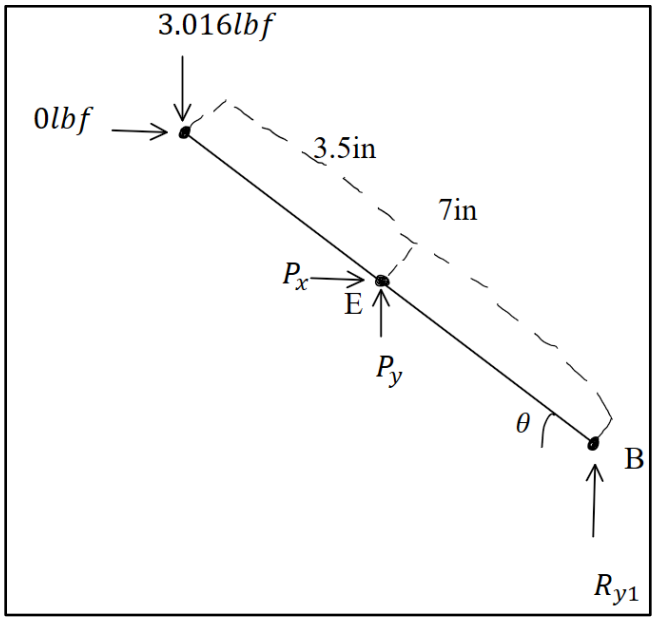

Figure 14: Free Body Diagram of First Arm

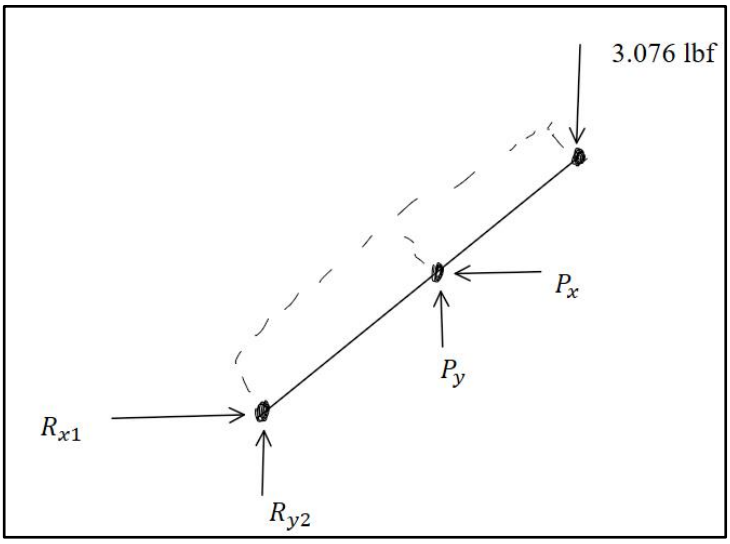

Figure 15: Free Body Diagram of Second Arm

4.2.2 - Min and Max force on bolts

When analysing the bolts we took into account the points at highest load shown in Figure 16-21. For our bolts we first calculated our stiffnesses where our youngs modulus (E) for aluminum is $10.3 * 10^6$psi, for steel $30 * 10^6$psi, and for PVC 474998.6 psi [5].There were 4 members for figure 13 which was two of the same plate and washer. The member stiffness of the plate was found using equation 1 which was found to be equal to $2528125.239 \frac{lbf}{in}$. The member stiffness of the washer was found using equation 2 and was found to be $181073029.6 \frac{lbf}{in}$. The total member stiffness can be calculated using

$$K_m = \left(\frac{2}{K_{plate}} + \frac{2}{K_{washer}}\right)^{-1} = 10594150.69 \frac{lbf}{in}$$

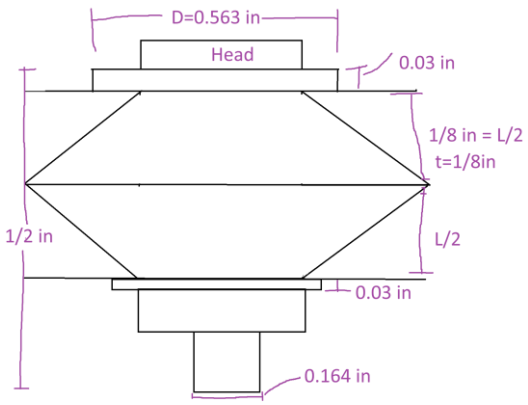

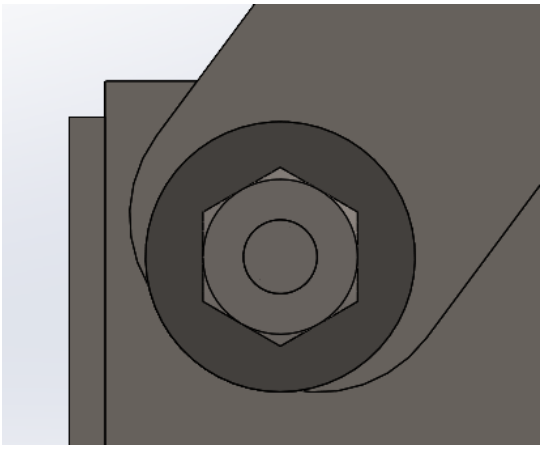

Figures 16 & 17: FBD of Rigid Scissor Lift Pivot

l_t shown in figure 16 equals $\frac{1}{2}in$ and $A_t = .01474in^2$ from table 8-2 in [5]. We can then plug in all of our values into equation 3 and get a total bolt stiffness of $884400\ \frac{lbf}{in}$. For figure 18 there are 5 members where 2 are the plate, 2 are the washer, and 1 is the pvc. The member of the plate was found using equation 1 and equals $2528125.239\frac{lbf}{in}$, the washer was found using equation 2 and equals $181073029.6\frac{lbf}{in}$, and the PVC was found using equation 1 but the youngs modulus for PVC was used which gave us $1106618.768\frac{lbf}{in^2}$. The total member was found using

$$K_m = \left(\frac{2}{K_{plate}} + \frac{2}{K_{washer}} + \frac{1}{K_{pvc}}\right)^{-1} = 1001958.548\frac{lbf}{in}$$

$$l_t = \frac{1}{2}in \qquad A_t = .01474in^2$$

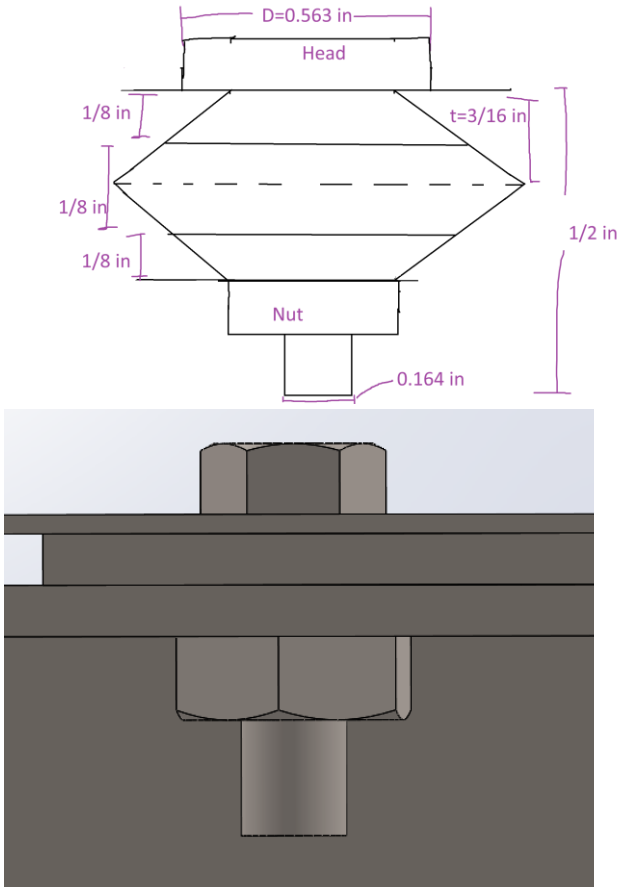

Figure 18 & 19: FBD of Bolt Fastening the Top Plate and Top Brackets

We then got our total bolt stiffness using equation 3 which equals $884400\frac{lbf}{in}$. For figure 17 there were 4 members involved which was 2 plates and 2 washers. The member for the plates were calculated using equation 1 and equals $2528125.239\frac{lbf}{in}$ and the member stiffness for the

washer were calculated using equation 2 and was found to be $181073029.6\frac{lbf}{in}$. The total member stiffness was found using

$$K_m = \left(\frac{2}{K_{plate}} + \frac{2}{K_{washer}}\right)^{-1} = 10594150.69\frac{lbf}{in}$$

$$l_t = \frac{3}{4}in \qquad A_t = .01474in^2$$

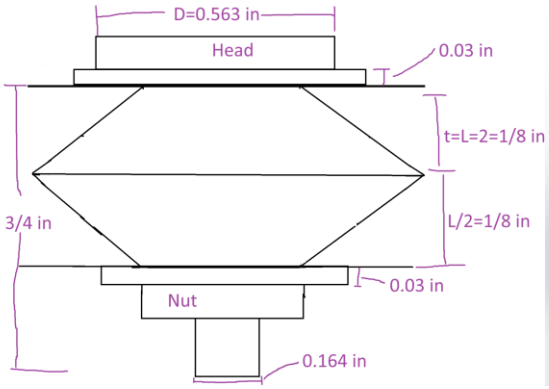

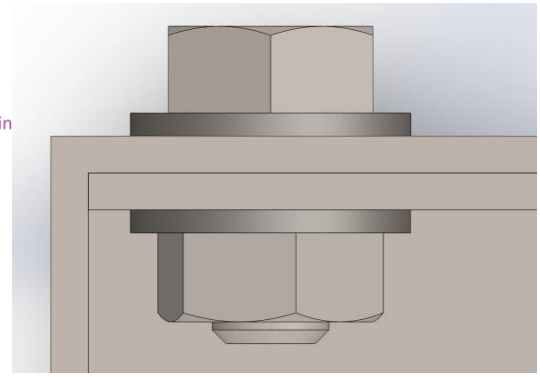

Figure 20 & 21: FBD of Bolt The Scissor Lift Body to the Legs.

Our total bolt stiffness was found using equation 3 and was found to be $589600\frac{lbf}{in}$.

$$K_{plate} = \frac{.5774*E_{Aluminum}*\pi*.164}{ln\left(\frac{(1.155t+D-d)(D+d)}{(1.155t+D-d)(D+d)}\right)} \quad \text{Eq 1}$$

$$K_{washer} = \frac{.5774\pi E}{2*ln\left(5*\frac{(.5774*l)+(.5d)}{(.5774*l)+(2.5d)}\right)} \text{ Eq 2}$$

$$K_b = \frac{A_t A_d E_{Steel}}{A_d l_t + A_t l_d} \quad \text{since } l_d = 0,\ K_b = \frac{A_t E_{Steel}}{l_t} \quad \text{Eq 3}$$

Our stiffness constants for all of our figures was found using equation 4 where for figure 13 $C = .077$ for figure 18 $C = .4688$, and for figure 20 $C = .37$.

$$C = \frac{k_b}{k_b + k_m} \quad \text{Eq 4}$$

We then calculated our torque on each bolt where we assumed that all 3 of our bolts will be under the same estimated torque. To find torque we first calculated $S_p = 0.85 * S_y$ where $S_y = 205 * 10^6\ MPa$ [6], $S_p = 174.25\ MPa\ or\ 25.273\ kpsi$. From these values we can then find $F_i = .75A_tS_p = 279.39\ lbf$. We can then find our torque which was $\tau = KF_id = 13.75\ lbf - in$ where $K = .3$ as we used nonplated machine screws [5]. Our max force shown in our Scissor lift calculations is equal to $P = 3.016\ lbf$. We then combined all of our values calculated above to find our min and max forces at each bolt shown in table 1.

Table 1: The min and max forces at each bolt

Figure number	$F_{bmin} = CP_{min} + F_i$ (lbf)	$F_{max} = CP_{max} + F_i$ (lbf)

16 and 17	279.3	279.622
18 and 19	279.3	280.803
20 and 21	279.3	280.505

4.3 - Bearing Design Force Analysis and Fitment Considerations

When tolerance fitting our bearings shown in figure 22 were fit into the wall as a tight tolerance fit against the wall and the shafts were tightly fit in the bearings. This means there were no external forces besides tolerance fits.

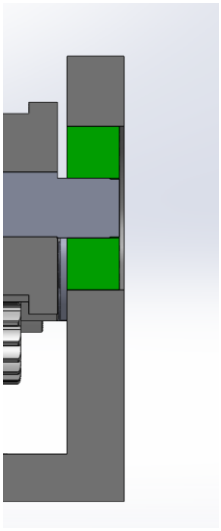

Figure 22

We know from our previous calculations above that the maximum force that is applied on our transmission walls when comparing it to the yield strength of the PLA plastic is not enough to compromise the material. Also due to the bearing force being in a single plane of motion we were able to print our frame in such a way to maximise strength in that plane's direction.

Moment of Walls From Bearings

$$M = \mu P \frac{d}{2} = .25 \text{ lbf-in} \qquad [7]$$

Maximum Force Applied to Transmission Walls

$$F = \frac{M}{d} = .278 \text{ lbf}$$

4.4 - Complete Force Analysis of Gear Train Shafts Under Dynamic Operation and Over Time

When first calculating for our gear train we took into consideration the torque we would get from our motor and the torque needed to lift the weight of 5lbs. The max torque we found

was .269lbf-in taking in consideration the max current of 2 amps. We also assumed that the environment did not affect our design whatsoever. We calculated the required torque to lift our gear train needs to lift the whole system to be 8 lbf-in (5lbs for the weight and 3lbs for the scissor lift and top plate). When finding our gear ratio we used our torque needed divided by the torque provided by the motor and got around 29.7:1 which can be rounded to 30:1. To split into different gears, we thought about just using 2 gears to amplify our torque but upon reflection the size of the 2 gears would have been impossible to fit within our size constraints. Due to this we decided to break it down into a total of 4 differently teethed gears and 6 Gears in total. The number of teeth these 4 different toothed gears we are using are 12, 24, 36, and 60 tooth gears. This gives us an amplification of 2x, 3x, and 5x which gives us a final Gear ratio of 30:1.

From taking the different gear tooth numbers we can find our torques and forces from table 2.

Number of Gear Teeth	Torques $T_{in} * \frac{N_G}{N_p} = T_{out}$	Forces $F = \frac{2T}{d_p}$
$N_1 = 12$	$T_1 = 0.269$lbf-in	$F_1 = 1.140$lbf
$N_2 = 24$	$T_2CCW = .538$lbf-in	$F_2 = 1.139$lbf
$N_3 = 12$	$T_3CCW = .538$lbf-in	$F_3 = 2.280$lbf
$N_4 = 36$	$T_4CW = 1.614$lbf-in	$F_4 = 2.278$lbf
$N_5 = 12$	$T_5CW = 1.614$	$F_5 = 6.839$lbf
$N_6 = 60$	$T_6CCW = 8.07$lbf-in	$F_6 = 6.833$lbf
The Pulley	$T_{Pulley}CCW = 8.07$lbf-in	$F_P = 16.14$lbf

Table 2: The Torques, Forces, and Number of Gear Teeth for the 6 Gears.

4.4.1 - Reaction Forces and Moments, Inertia, and Deflections of Shafts

When calculating for our shafts we ordered them as shown in figure 31 and 24.

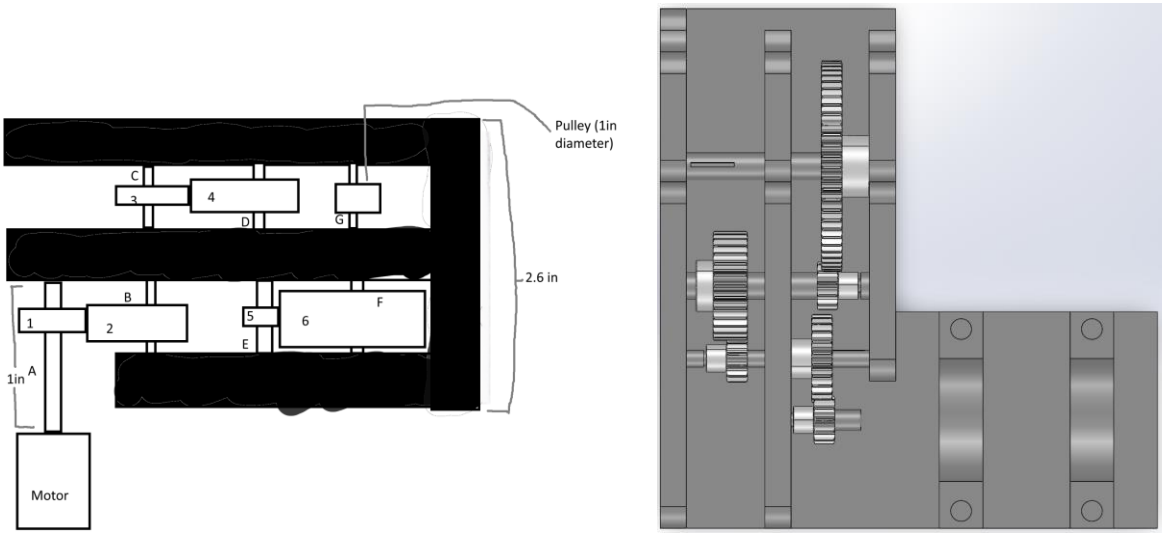

Figure 23 & 24: Top View of Gear Train Setup

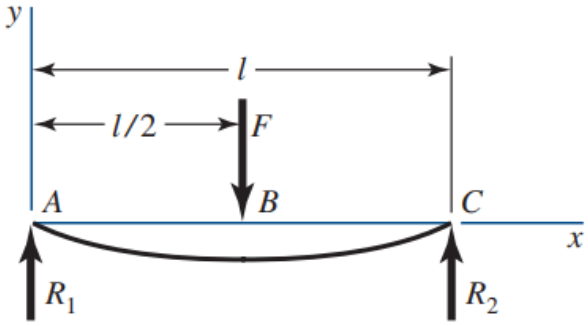

Figure 25: Example diagram from table A-9,5 [5]

Table 3: Forces and moments of our shafts

Shaft	$R_1 = R_2 = \frac{F}{2}$	$M_1 = M_2 = \frac{FL}{8}$	$I = \frac{\pi d^4}{64}$
A	$0.570\ lbf$	$0.185\ lbf * in$	$3.217 * 10^{-5}\ in^4$
B	$0.569\ lbf$	$0.142\ lbf * in$	$7.854 * 10^{-5}\ in^4$
C	$1.140\ lbf$	$0.285\ lbf * in$	$7.854 * 10^{-5}\ in^4$
E	$3.419\ lbf$	$0.855\ lbf * in$	$4.533 * 10^{-4}\ in^4$
F	$3.417\ lbf$	$0.854\ lbf * in$	$4.533 * 10^{-4}\ in^4$
G	$8.070\ lbf$	$2.018\ lbf * in$	$4.533 * 10^{-4}\ in^4$

Our max deflection for shaft A was found to be where our youngs modulus was $1106618.768\frac{lbf}{in^2}$[5] and using table A-9,5

$$y_{max} = \frac{-F_1 {L_A}^3}{192EI} = -6.67 * 10^{-4}\ \text{in}$$

Our shear and moment diagrams for shaft A are shown below.

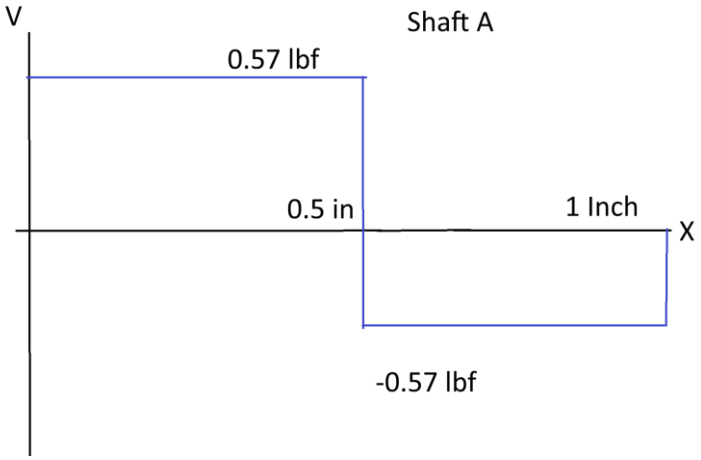

Figure 26: Shear Diagram of Transmission Shaft A

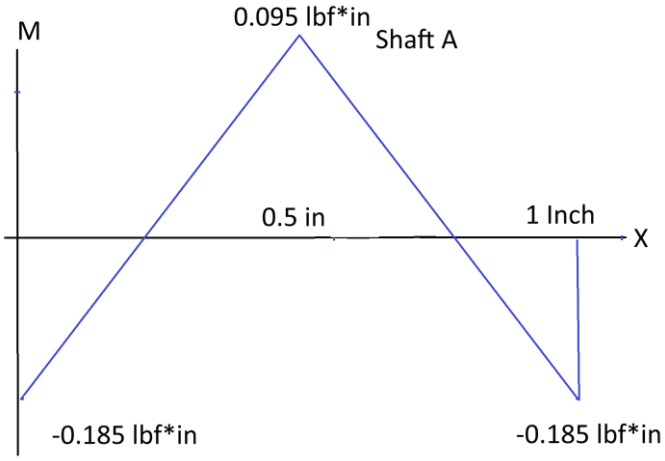

Figure 27: Moment Diagram of Transmission Shaft A

For shaft B-C we calculated the deflection by separating our shaft into 3 parts and calculated through super position. The first part from the 24 tooth gear where the equation was from table A-9, 6 where we got was

$$y_{F1} = \frac{Fbx}{6EIl}(x^2 + b^2 - l^2) = .00269\text{in}$$

Our second deflection from the middle wall was from table A-9,5[5] where we got

$$y_{F2} = -\frac{Fl^3}{48IE} = -.0072\text{in}$$

our third deflection was from from the 12 tooth gear table A-9,6 [5] where we got

$$y_{F3} = \frac{Fbx}{6EIl}(x^2 + b^2 - l^2) = .0054\text{in}$$

our total deflection for shaft B-C was

$$y = y_{F1} + y_{F2} + y_{F3} = 9 * 10^{-4}\text{in}$$

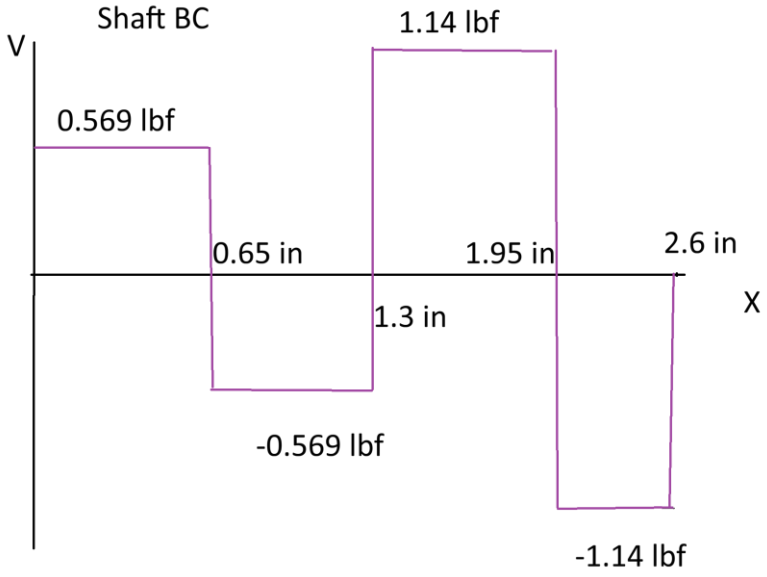

Figure 28: Shear Diagram of Transmission Shaft B-C

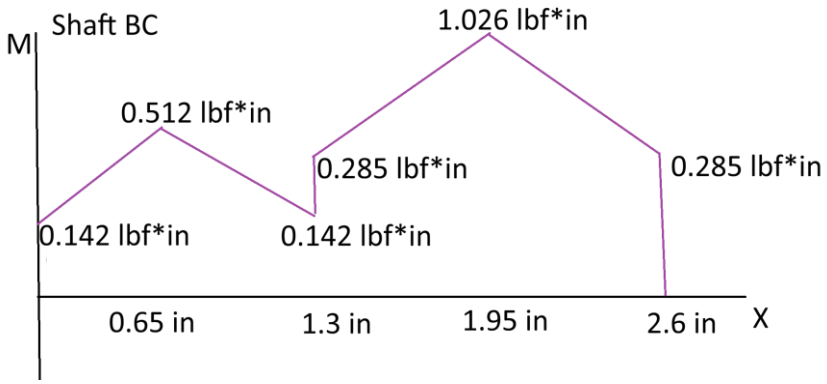

Figure 29: Moment Diagram of Transmission Shaft B-C

For shaft D-E we calculated the deflection by separating our shaft into 3 parts and calculated through super position. The first part from 36 tooth where the equation is from table A-9, 6 where we got

$$y_{F1} = \frac{Fbx}{6EIl}(x^2 + b^2 - l^2) = -.0132\text{in}$$

Our second deflection from the middle wall from with equation from table A-9,5[5] where we got

$$y_{F2} = -\frac{Fl^3}{48IE} = -.0235\text{in}$$

our third deflection was from 12 tooth where the equation was from table A-9,6 [5] where we got

$$y_{F3} = \frac{Fbx}{6EIl}(x^2 + b^2 - l^2) = -.001\text{in}$$

our total deflection for shaft D-E was

$$y = y_{F1} + y_{F2} + y_{F3} = -.0379\text{in}$$

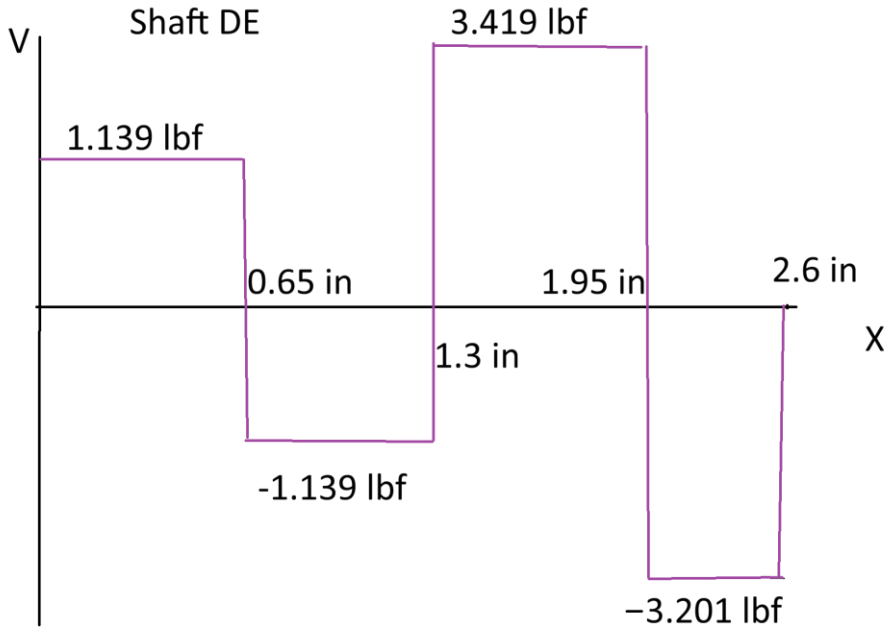

Figure 30: Shear Diagram of Transmission Shaft D-E

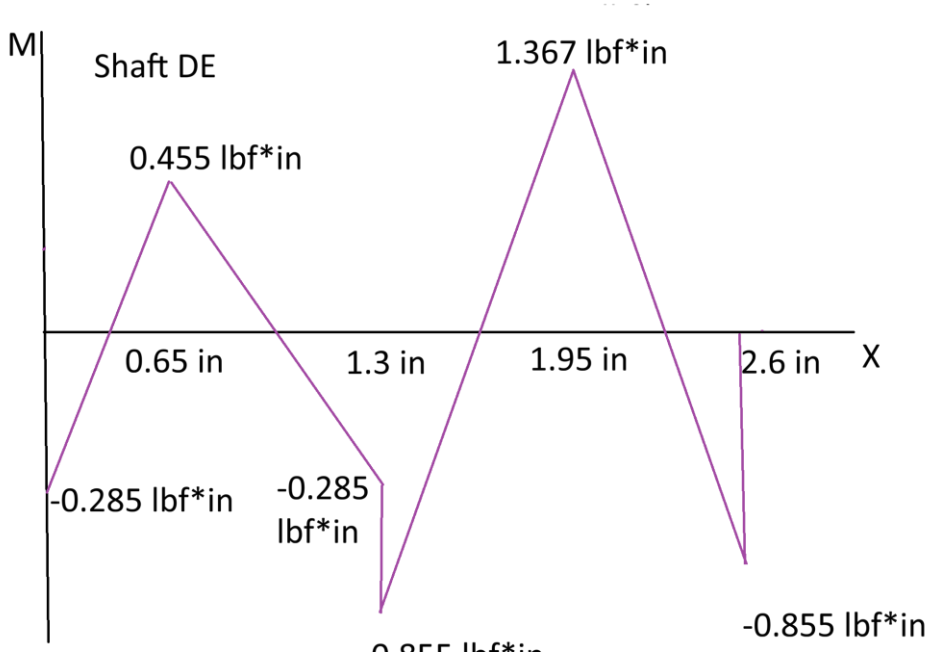

Figure 31: Moment Diagram of Transmission Shaft D-E

For shaft F-G we calculated the deflection by separating our shaft into 3 parts and calculated through super position. The first part was the 60 tooth where the equation was from was from table A-9, 6 where we got

$$y_{F1} = \frac{Fbx}{6EIl}(x^2 + b^2 - l^2) = .0395\text{in}$$

Our second deflection was the middle wall where the equation was from table A-9,5[5] where we got

$$y_{F2} = -\frac{Fl^3}{48IE} = -0.1181\text{in}$$

our third deflection was the pulley where our equation was from table A-9,6 [5] where we got

$$y_{F3} = \frac{Fbx}{6EIl}(x^2 + b^2 - l^2) = -.1181\text{in}$$

our total deflection for shaft F-G was

$$y = y_{F1} + y_{F2} + y_{F3} = .0148\text{in}$$

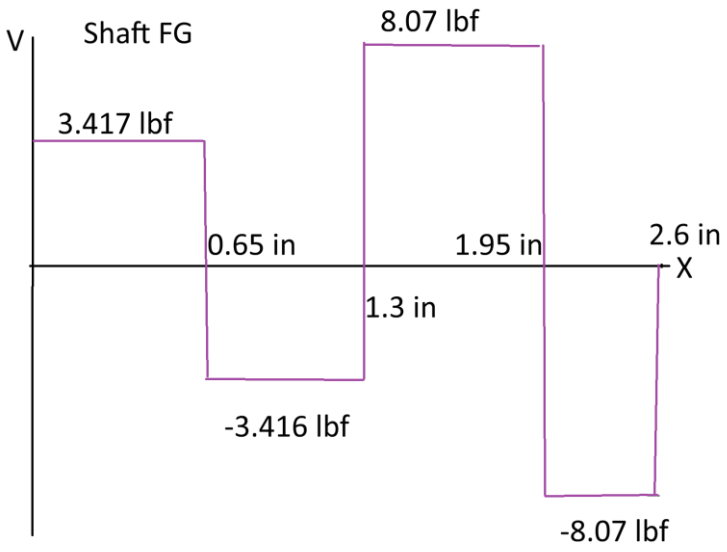

Figure 32: Shear Diagram of Transmission Shaft F-G

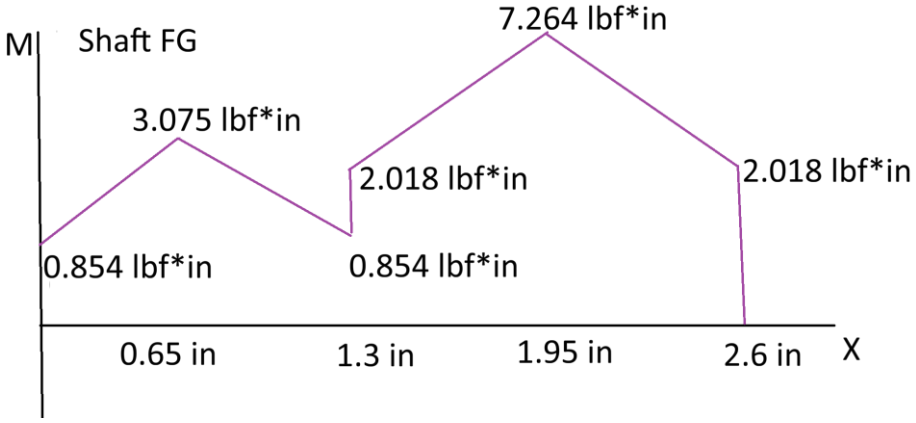

Figure 33: Moment Diagram of Transmission Shaft F-G

4.4.2 - Gear Train Shaft Tolerances

For all of the holes and shafts in both the transmission and bracket, we are using a clearance close running fit. This means that the "symbols" we are using are from table 7-9 H8/f7 [5] . In all cases, the diameter of the hole, D, and shaft, d, are equal ($D = d$). When calculating our tolerance grades for the holes and shafts were found in table A-13 to be

$$\Delta D = 0.0007 \text{ in and } \Delta d = 0.0005 \text{ in [5]}$$

our deviation was found through table A-14 to be

$$\delta_F = -0.0004 \text{ in [5]}$$

We can then find our diameter for the hole and the shaft

$$D = d = D_{min} = 0.16 \text{ in}$$
$$D_{max} = D + \Delta D = 0.1607 \text{ in}$$
$$d_{max} = d + \delta_F = 0.1596 \text{ in}$$
$$d_{min} = d + \delta_F - \Delta d = 0.1591 \text{ in}$$

For our other small transmission of .2 inches we found our tolerance grades through table A-13 $\Delta D = 0.0007$ in and $\Delta d = 0.0005$ in [5]

our deviation was found through table A-14

$$\delta_F = -0.0004 \text{ in [5]}$$

our diameter for our holes and shafts were then found

$$D = d = D_{min} = 0.2 \text{ in}$$
$$D_{max} = D + \Delta D = 0.2007 \text{ in}$$
$$d_{max} = d + \delta_F = 0.1996 \text{ in}$$
$$d_{min} = d + \delta_F - \Delta d = 0.1991 \text{ in}$$

For our larger transmission of .31 inches we found our tolerance grades from table A-13

$$\Delta D = 0.0009 \text{ in and } \Delta d = 0.0006 \text{ in [5]}$$

our deviation was found through table A-14

$$\delta_F = -0.0005 \text{ in [5]}$$

our diameters were then found from these values

$$D = d = D_{min} = 0.31 \text{ in}$$
$$D_{max} = D + \Delta D = 0.3109 \text{ in}$$
$$d_{max} = d + \delta_F = 0.3095 \text{ in}$$
$$d_{min} = d + \delta_F - \Delta d = 0.3089 \text{ in}$$

The diameter of the holes and shafts in the brackets were around 0.24 inches. We found our deviations from table A-13.

$$\Delta D = 0.0009 \text{ in and } \Delta d = 0.0006 \text{ in [5]}$$

we then found our deviations from table A-14.

$$\delta_F = -0.0005 \text{ in[5]}$$

from these we can find our diameters

$$D = d = D_{min} = 0.24 \text{ in}$$
$$D_{max} = D + \Delta D = 0.2409 \text{ in}$$
$$d_{max} = d + \delta_F = 0.2395 \text{ in}$$
$$d_{min} = d + \delta_F - \Delta d = 0.2389 \text{ in}$$

4.4.3 - Max Stress Concentration Calculations For Gears

When calculating the stress concentration factors for our gears using table A-15 looking at Figure 1 and 8. [5] We found the stress concentration for the 12-24 tooth mesh where our x and y were

$$(r/d) = 0.25, (D/d) = 1.25$$

respectively which gave our max stress concentration to be 1.19. For our 12-36 tooth our x and y values respectfully were

$$(r/d) = 0.5, (D/d) = 1.5$$

which gave us a max stress concentration value of 1.19. Since the 12-60 tooth and 12-36 tooth shafts are made from the same material and are the same dimensions, their maximum stress concentration values are equal.

4.4.4 - Estimated number of Life Cycles for each Transmission Shaft

To determine the fatigue failure criteria we used two different methods of Goodman and Smith-Watson-Topper (SWT). The Goodman failure criteria provides the most basic and universal finite cycle evaluations. Along with this there isn't any specific class of material this fatigue method was created for like other fatigue testing methods so it will be the best fit for the nylon shafts we are using. The SWT Fatigue criteria because our system matches many of the Pros it has to offer. These are that we have a low level of fatigue with our high total life cycles and that we experience a very small level of plastic deformation due to our shaft being fixed on each end severely limiting any form of plastic deformation that could occur. It is also good at predicting failure under a completely reversible load, like that of the arms. Our calculations are shown in table 4.

Table 4

Shafts	τ_m Psi	τ_a Psi	SWT method $n_f = \frac{S_e}{\sqrt{(\tau_m+\tau_a)\tau_a}}$	Goodman Method $n_f = (\frac{\tau_a}{S_e} + \frac{\tau_m}{S_{ut}})^{-1}$
A	46.155	46.155	12.27	16.06
B and C	149.04	149.04	3.80	4.97
D and E	158.115	158.115	3.58	4.69
F and G	424.02	424.02	1.34	1.75

The equations for the life cycle of the transmission shafts are calculated from using stress-life coefficient data denoted as reference [1], as there was no data for the fatigue strength coefficient. The equations are:

$$S_f = aN^b, \text{ where } a = 395.67, b = -0.3831, S_f = \tau_a, N = (\frac{S_f}{a})^{-\frac{1}{b}}$$

Using the alternating stress in table 4 for each shaft in the vertical orientation:

$N_a = 272.8E3, N_b = 12.79E3 = N_c, N_d = 10.96E3 = N_e, N_f = 0.83E3 = N_g$ Cycles before failure (subscript denotes each shaft's life).

4.5 - Specific Materialistic and Budgetary Design Decisions

The acetal gears were chosen because they had the necessary number of teeth, while being lightweight and affordable. The weight of the gears range from 0.0024 lbs to 0.039lbs, which minimizes deflection and reaction forces on the shafts. The Shafts were designed using PLA from a 3D printer because it was the cheapest, most available material that doesn't cause significant deflection, as well as having a high flexural strength of 580000 psi, which was a little higher than other materials that were considered, but were too difficult or expensive to procure.

The gear frame was made of PLA because it was available, while being able to hold the weight of the gear train.

4.6 - Bill of Materials(BOM) Documentation

Detailed supporting documentation for the final design is provided in the appendix section. The complete Bill of Materials, including part names, quantities, costs, sources, and URLs, is included in Appendix B. The electronics schematics for the motor and power system is included in Appendix C.

4.7 - Designated Design Challenges that Must be Overcome

The final scissor lift system was designed, analyzed, fabricated, and demonstrated in compliance with the complete set of requirements outlined in the ENME 304 Lift Platform Challenge rules, not solely the bolded demonstration scoring criteria.

Dimensional requirements were satisfied by ensuring the device began operation at a height below 8 inches. The device also remained fully self-standing within an 8in by 8in area and could successfully extend to the 12 inch finish line without being attached to the supporting surface.

Electrical and Power requirements were met through the exclusive usage of the provided Mabuchi RS-555PH-3255 DC motor and 12 V battery pack. A DPDT forward-reverse circuit with a protective diode and a 2 amp slow-blow fuse was implemented with no additional electronic or power sources. The system operated within the specified current limits and the battery was not recharged during the demonstration hours.

Drive system requirements were also satisfied through the usage of a custom gear and pulley drivetrain designed and fabricated from individual components as opposed to pre-built gearboxes and commercial kits. All rotating shafts were supported by bearings, bearings were loaded only in their intended directions, and all gears and pulleys were mechanically secured to shafts using an approved fastening method. There was no stored mechanical energy anywhere in the system and alignment was carefully controlled through careful and precise assembly.

Construction requirements were addressed by selecting appropriate non-wood materials for the structure and drivetrain, incorporating rapidly-prototyped and machined components, and ensuring a complete model of the device in CAD(Figure 2). The team number was also clearly displayed on the final device.

Safety requirements were addressed by adhering to standard shop safety practices during fabrication and assembly, maintaining controlled operating speeds, and ensuring all rotating components were supported and aligned.

Demonstration requirements were considered when designing the system to ensure complete lifting and resetting of the device within the specified time limits and reliable operation under repeated trails. During the final assembly immediately prior to testing however, a failure occurred in the final output shaft connecting the largest gear to the pulley driving the scissor lift. This component's failure was due to a local design weakness rather than a system-level failure of the drivetrain. All other components were functional and properly aligned.

Budget requirements were satisfied by selecting components and materials that met performance needs whilst remaining within the given budget. All purchases were approved through the official procurement processes and the complete Bill of Materials documenting cost, quantity, source, and justification is included within the Appendix.

Sustainability requirements were addressed by designing the system to be easily disassembled, allowing for reusable components at the end of the project. Components were assembled using mechanical fasteners rather than permanent bonding methods to ensure reusability.

4.7.1 - Specialized Design Processes and Execution

For our final design, our machined parts were our Scissor Lift Arms and the L-Brackets that provided the support for our load and the frame (or structure) for our design. We ordered enough material to have some test cuts, allowing us to practice our machining on these parts first. Once this was done and we had finalized our dimensions and machining process, we began machining our parts. To manufacture the scissor lift arms, they were bound together with tape and clamps with the top beam marked for drilling. We drilled all of the arms at once to ensure we had equal hole alignment in all of the arms without deviation, meaning that each of the arms had symmetry. We also drilled opposing L-Brackets together so there would be minimal deviation in these holes. This is especially important for the pivots of our scissor lifts which need to be accurately placed or else our system may lose stability from them being offset or our system might get caught up on itself.

Our design required a significant amount of 3D printing which allowed us to make rapid changes and fixes whenever it is required. This was crucial to our project because upon assembly of our system, we had many small dimensional errors which had to be fixed. One of which was getting the timing teeth right on our pulleys. This took until the 3rd iteration to get right, however once it had been corrected we had a nice tight fit allowing us to have relatively no slip. Our other rapidly prototyped parts were our gear train and the battery and switch mount. It was crucial that we were able to print multiple Gear Train Frames because it took us 5 prints to get our Bearing fitment right

5. Discussion

5.1 - Post Demonstration Evaluation and System Evaluation

The scissor lift had a decent performance in terms of assembly and modification, but failed to work because one shaft failed. That shaft was poorly designed because it relied on a thin PLA pin, which was too thin and weak, to connect the shaft between the largest gear and the driver pulley, and broke during insertion. There wasn't any planned distance for the pulley driver and pinion either. There were also problems with tolerancing parts. There are many possible improvements for each of these issues. One possible solution for the shaft would be to replace the PLA shafts with 6061T6 aluminum, so they would be much stronger in compression. Another solution would be to design the last shaft, so it wouldn't rely on a PLA key. A possible solution for the tolerancing on the gear frame would be to separate each wall into two portions along the center of the holes, then put in machine screws on the ends of the frame with nuts to tighten both portions together. This could also be improved further by printing each wall separately and securing them with 3D printed inserts to allow for simpler and more accurate 3D printing.

5.2 - System Accessibility and Modularity

A key feature of the scissor lift is its ease of assembly and modification to the body. The scissor arms were resting on top of the brackets on one side, allowing the platform and arms to act as a lid when the pulley wasn't installed. This design allowed simple assembly of the gear train, frame, switch, and electrical system, as well as the arms and platform. Each of these components are secured with screws or shaped cavities. This allows for easy, non-destructive disassembly of parts, as well as the reuse of most parts, such as the bearings, gears, and brackets. The only parts that aren't reusable are the 3D printed parts because they are toleranced to specific length specifications and it wouldn't be smart to reuse PLA stepdown shafts because PLA isn't very strong and stepdown shafts have increased stress at the step.

5.3 - Post Design Reflections and Takeaways

From this project, there are two main conclusions. The first conclusion is that the tolerance of custom parts should be more thoroughly considered when undergoing the designing process. The manufacturing methods for the shafts and frame couldn't reliably make parts in the planned tolerances for them, so these parts were repetitively 3D printed multiple times in the week leading to the demonstration because they were built around a tight tolerance in the ten-thousandths of an inch. The second conclusion is that the calculations are theoretical and don't account for real-world factors in the actual design as opposed to ideal conditions. In calculations, friction was ignored between the gears and between the bearings and shafts. During a test of the gear train, it was observed that the gears weren't spinning as fast as expected. All the ignored

factors were lessening the output speed and torque of the gears. Although it still has enough torque and speed, that caught the team off-guard.

6. Reference

[1] Azadi, M, et al. “High-Cycle Bending Fatigue Properties of Additive-Manufactured ABS and PLA Polymers Fabricated by Fused Deposition Modeling 3D-Printing.” *Science Direct*, 22 Jan. 2021, Accessed 17 Dec. 2025.

[2] “Polylactic Acid (PLA, Polylactide).” *Polylactic Acid (PLA, Polylactide) :: MakeItFrom.Com*, 30 May 2020, www.makeitfrom.com/material-properties/Polylactic-Acid-PLA-Polylactide.

[3] “KHK DS1-12, Module 1, 12 Tooth, Injection Molded Spur Gears.” *KHK*, KHK, www.khkgears.us/catalog/product/DS1-12/. Accessed 13 Dec. 2025.

[4] “KHK DS1-60, Module 1, 60 Tooth, Injection Molded Spur Gears.” *KHK*, KHK, www.khkgears.us/catalog/product/DS1-60/. Accessed 13 Dec. 2025.

[5] Nisbett, J. Keith, and Budynas, Richard G.,“*Shigley’s Mechanical Engineering Design”, 2024 Edition*, McGraw Hill LLC, New York, NY, 2024

[6] “18-8 stainless steel,” Xometry Materials Resource. Available: https://www.xometry.com/resources/materials/18-8-stainless-steel/. Accessed: Nov. 24, 2025.

[7] JTEKT, “Frictional coefficient (reference) | Basic Bearing Knowledge | Koyo Bearings /JTEKT CORPORATION,” koyo.jtekt.co.jp. https://koyo.jtekt.co.jp/en/support/bearing-knowledge/8-4000.html

[8]“T I M I N G 40DP 40DP 40DP Belts.” Accessed: Dec. 18, 2025. [Online]. Available: https://www.ondrivesus.com/documents/categories/timing-belts-all-series.pdf

7. Appendix

GANTT CHART

PROJECT TITLE	Lift Platform Challenge
MEMBERS NAMES	Bilal Faizullah, John Xavier, Ian Wright, Adam
CLASS NAME	ENME 304: Machine Design
PROJECT LENGTH	08/27/25 - 12/15/25

	TASK TITLE	TASK LEADER	IDEAL OR ASSIGNED START DATE	IDEAL END OR DUE DATE	PERCENT OF TASK COMPLETE
1	**Introduction & Conception**				
1.1	Course Introduction	N/A	8/27/25	9/2/25	100%
1.2	Project Introduction	N/A	9/3/25	9/22/25	100%
1.3	Group Creation	N/A	9/22/25	9/22/25	100%
1.4.1	Brainstorming Session	Adam	9/22/25	9/24/25	100%
1.4.2	Revision & Narrowing of Concepts	Ian	9/24/25	9/26/25	100%
2	**Definition & Planning**				
2.1	Rule and Specs Review	Adam	9/27/25	9/27/25	100%
2.2	Creation of Gantt Chart	Bilal	9/27/25	9/29/25	100%
2.3	Search for supplier	John	9/27/25	9/27/25	100%
2.4	Elaboration of Concepts	Ian	9/27/25	9/29/25	100%
2.5	Evaluation of Concepts	Adam	9/27/25	9/29/25	100%
2.6	Submission of Design Update 1	Bilal	9/30/25	9/30/25	100%
2.9	Concept for a Prototype	Ian	10/1/25	10/3/25	100%
3	**Creation**				

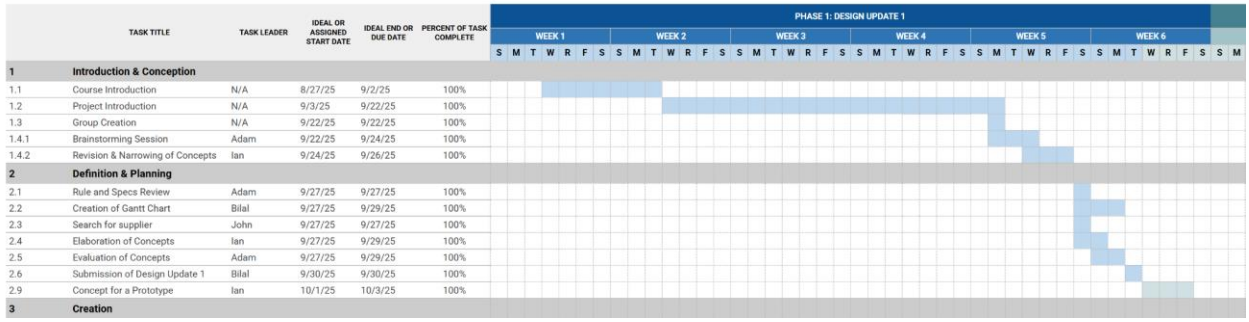

Figure A1: First part of the Gantt Chart

GANTT CHART

PROJECT TITLE	Lift Platform Challenge
MEMBERS NAMES	Bilal Faizullah, John Xavier, Ian Wright, Adam
CLASS NAME	ENME 304: Machine Design
PROJECT LENGTH	08/27/25 - 12/15/25

	TASK TITLE	TASK LEADER	IDEAL OR ASSIGNED START DATE	IDEAL END OR DUE DATE	PERCENT OF TASK COMPLETE
3	**Creation**				
3.1	Prototype CAD Models	John	10/3/25	10/10/25	100%
3.2.2	Conceptualize Rapid-Prototyped & Machined Parts	Bilal	10/5/25	10/7/25	100%
3.2.3	Rework Prototype Concept	Ian	10/7/25	10/19/25	100%
3.3	Begin Bill of Materials	Bilal	10/8/25	10/9/25	100%
3.4.1	Prep of Prelim Design Review	Adam	10/10/25	10/19/25	100%
3.4.2	PDR Presentation	Ian	10/20/25	10/20/25	100%
3.4.3	Incorporation of PDR Feedback	John	10/21/25	10/31/25	100%
3.5	"Final" Design Calculations	Adam	10/22/25	10/26/25	100%
3.6	Submission of Design Update 2	Bilal	10/28/25	10/28/25	100%
3.7.1	Selection of Final Project	Adam	10/29/25	10/30/25	100%
3.7.2	Final CAD Model	John	10/31/25	11/9/25	100%
3.8	Detailed Description of Final Project	Ian	10/31/25	11/15/25	100%
3.10.1	Order Materials	Bilal	11/1/25	11/19/25	100%
3.9	Submission of Design Update 3	Bilal	11/24/25	11/24/25	100%

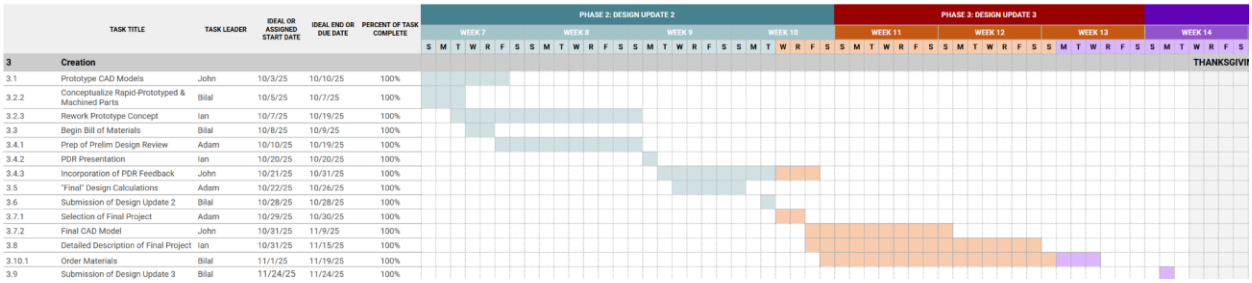

Figure A2: Second part of the Gantt Chart

GANTT CHART

PROJECT TITLE	Lift Platform Challenge
MEMBERS NAMES	Bilal Faizullah, John Xavier, Ian Wright, Adam
CLASS NAME	ENME 304: Machine Design
PROJECT LENGTH	08/27/25 - 12/15/25

	TASK TITLE	TASK LEADER	IDEAL OR ASSIGNED START DATE	IDEAL END OR DUE DATE	PERCENT OF TASK COMPLETE
3	**Creation**				
3.9	Submission of Design Update 3	Bilal	11/24/25	11/24/25	100%
3.10.2	Prototyping Final Project	Adam	11/1/25	12/02/25.	100%
3.10.3	Bill of Materials	Bilal	11/1/25	11/25/25	100%
3.11.	Final Report Drafting	Adam	11/19/25	11/25/25	100%
4	**Performance & Reiterations**				
4.1	Rules and Regulations Check	Adam	11/24/25.	12/3/25	100%
4.2	Trial Runs	Bilal	11/24/25	12/3/25	100%
4.3	Final Report Completing	John	12/1/25	12/15/25	100%
4.4	Check Compliance With Project Requirements	John	12/3/25	12/3/25	100%
4.5	Presentation Prep	Adam	12/4/25	12/7/25	100%
4.6	Project Demonstration; Disassembly	Ian	12/8/25	12/8/25	100%
4.7	Final Report Submission	Bilal	12/15/25	12/15/25	100%

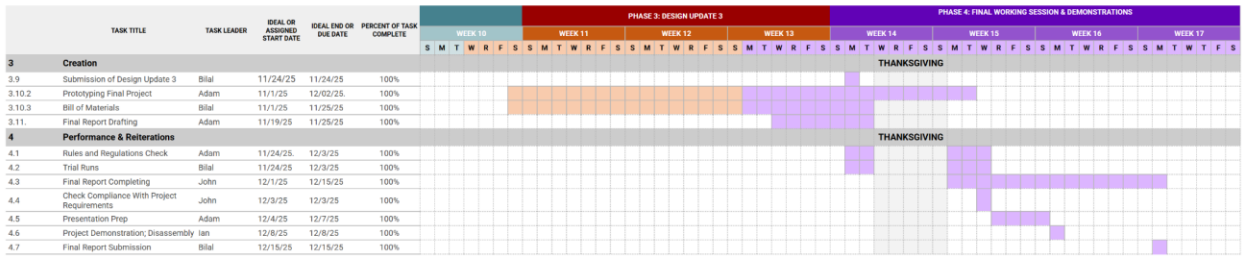

Figure A3: Third part of the Gantt Chart

	Item Name	Item Description	3D Print Volume	Individual Cost	Quantity Needed	Total Cost
1	Multipurpose 6061 Aluminum 90 Degree Angle	1" ht, 1" wd 1/8" thick 90 deg. 8ft long	N/A	$19.50	1	$19.50
2	18-8 Stainless Steel Washer	Spacer for Pivots under motion	N/A	$7.81 pack of 100	1 pack	$7.81
3	Zinc-Plated Low-Strength Steel Hex Nuts	8-36 threaded nut	N/A	$3.17 pack of 100	1 pack	$3.17
4	Passivated 18-8 Stainless Steel Pan Head Phillips Screw	Machine Screw For Holding our Device together	N/A	$8.25 Pack of 25	1 pack	$8.25
5	12 Tooth Plastic Gear	12 tooth Plastic Spur Gear	N/A	$4.30	3	$12.90
6	24 Tooth Plastic Gear	24 tooth Plastic Spur Gear	N/A	$4.33	1	$4.33
7	36 Tooth Plastic Gear	36 tooth Plastic Spur Gear	N/A	$5.60	1	$5.60
8	60 Tooth Plastic Gear	60 tooth Plastic Spur Gear	N/A	$8.81	1	$8.81
9	Moisture- and Wear-Resistant Nylon Rod	Gear Shaft Machined down to Proper size, 1ft	N/A	$6.72	1	$6.72
10	Aluminum Metal Bar	4 ft Aluminum Bar for Scissor Lift Arms 1-1/4in wide 1/8th in thick	N/A	$12.50	1	$12.50
11	Barrel Extension 7/8 in	7/8inch 8-32 thread Entention for Barrel of Axle	N/A	$3.85	3	$11.55
12	Machine Screw 12-24 1/2 inch long	Machine Screw For Holding our Device together	N/A	$6.93 pack of 25	1	$6.93
13	Low Profile Barrel and Screw	5 inch long 8-32 thread Barrel and screw for Pully/Spool Axle	N/A	$6.87	4	$27.48
14	Barrel Extension 3/4 in	3/4inch 8-32 thread Entention for Barrel of Axle	N/A	$3.76	1	$3.76
15	Fishing line	Pulls spool	N/A	$4.59	1	$4.59
16	Chemical Resistant PVC Sheet	12x12", 1/8" thick For top plate	N/A	$8.76	1	$8.76
17	Sloblo Fuse	2A fuse pack of 20	N/A	6.99	1	6.99
18	DPDT Switch	6 pins	N/A	$2.47	1	$2.47
19	Fuse Holder	Fit Slo blo Fuse pack of 5	N/A	$5.19	1	$5.19
20	PLA Plastic	Creality 2kg Black & White PLA 1.75mm Filament Bundle for 3D F	N/A	$25.49	1	$25.49

Figure B1: First half of the Bill of Materials

	Item Name	Ordered	Arrived	Material	Part #	Supplier	URL
1	Multipurpose 6061 Aluminum 90 Degree Angle	☑	☑	6061 Aluminum	8982K4	McMaster	https://www.mcmaster.com/8982K4-8982K21/
2	18-8 Stainless Steel Washer	☑	☑	Carbon Steel	92141A223	McMaster	https://www.mcmaster.com/92141A223/
3	Zinc-Plated Low-Strength Steel Hex Nuts	☑	☑	Zinc Plated Steel	90480A185	McMaster	https://www.mcmaster.com/90480A185/
4	Passivated 18-8 Stainless Steel Pan Head Phillips Screw	☑	☑	Stainless Steel	91772A925	McMaster	https://www.mcmaster.com/91772A925/
5	12 Tooth Plastic Gear	☑	☑	Durcan Acetal M90-44 Plastic	DS1-12	KHK	https://www.khkgears.us/catalog/product/DS1-12/
6	24 Tooth Plastic Gear	☑	☑	Durcan Acetal M90-44 Plastic	DS1-24	KHK	https://www.khkgears.us/catalog/product/DS1-24/
7	36 Tooth Plastic Gear	☑	☑	Durcan Acetal M90-44 Plastic	DS1-36	KHK	https://www.khkgears.us/catalog/product/DS1-36/
8	60 Tooth Plastic Gear	☑	☑	Durcan Acetal M90-44 Plastic	DS1-60	KHK	https://www.khkgears.us/catalog/product/DS1-60/
9	Moisture- and Wear-Resistant Nylon Rod	☑	☑	Nylon	8641T52	McMaster	https://www.mcmaster.com/8682K83/
10	Aluminum Metal Bar	☑	☑	6063 Aluminum	89755K31	McMaster	https://www.mcmaster.com/89755K31-89755K311/
11	Barrel Extension 7/8 in	☑	☑	18-8 Stainless Steel	93122A117	McMaster	https://www.mcmaster.com/93122A117/
12	Machine Screw 12-24 1/2 inch long	☑	☑	Steel	91772A923	McMaster	https://www.mcmaster.com/91772A923/
13	Low Profile Barrel and Screw	☑	☑	18-8 Stainless Seel	94887A251	McMaster	https://www.mcmaster.com/94887A251/
14	Barrel Extension 3/4 in	☑	☑	18-8 Stainless Seel	93122A116	McMaster	https://www.mcmaster.com/93122A116/
15	Fishing line	☑	☑	Nylon	B09N72VZGW	Amazon	https://a.co/d/9v8UW7j
16	Chemical Resistant PVC Sheet	☑	☑	PVC Type 1	8747K112	McMaster	https://www.mcmaster.com/8747K112/
17	Sloblo Fuse	☑	☑	N/A	B07X3GFV8K	Amazon	https://a.co/d/8z74kEH
18	DPDT Switch	☑	☑	N/A	EG5646-ND	Digikey	https://www.digikey.com/short/nmt8hfjv
19	Fuse Holder	☑	☑	N/A	B00H3CVSXQ	Amazon	https://a.co/d/3ZTMF1t
20	PLA Plastic	☑	☑	PLA Plastic	B0C4TNQZYY	Amazon	https://a.co/d/4kG0Vdi

Figure B2: Second half of the Bill of Materials

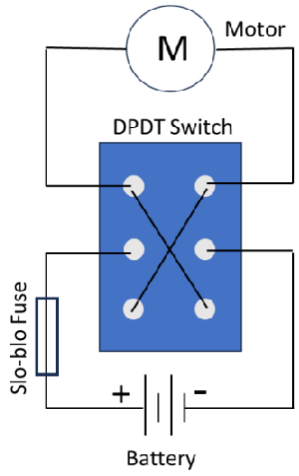

Figure C1: DPDT Electrical Circuit/Schematic

7.1 - The Torques, Forces, and Number of Gear Teeth for the 6 Gears.

Number of Gear Teeth	Torques $T_{in} * \frac{N_G}{N_p} = T_{out}$	Forces $F = \frac{2T}{d_p}$
$N_1 = 12$	$T_1 = 0.269$lbf-in	$F_1 = \frac{2T_1}{d_{p1}} = \frac{2*.269}{.472} = 1.140$lbf
$N_2 = 24$	$T_2CCW = T_1 * \frac{N_G}{N_p} = .269 * \frac{24}{12} = .538$lbf-in	$F_2 = \frac{2T_2}{d_{p2}} = \frac{2*.538}{.945} = 1.139$lbf
$N_3 = 12$	$T_3CCW = T_1 * \frac{N_G}{N_p} = .269 * \frac{24}{12} = .538$lbf-in	$F_3 = \frac{2T_3}{d_{p3}} = \frac{2*.538}{.472} = 2.280$lbf
$N_4 = 36$	$T_4CW = T_3 * \frac{N_G}{N_p} = .538 * \frac{36}{12} = 1.614$lbf-in	$F_4 = \frac{2T_4}{d_{p4}} = \frac{2*1.614}{1.417} = 2.278$lbf
$N_5 = 12$	$T_5CW = T_3 * \frac{N_G}{N_p} = .538 * \frac{36}{12} = 1.614$	$F_5 = \frac{2T_5}{d_{p5}} = \frac{2*1.614}{.472} = 6.839$lbf
$N_6 = 60$	$T_6CCW = T_5 * \frac{N_G}{N_p} = 1.614 * \frac{60}{12} = 8.07$lbf-in	$F_6 = \frac{2T_6}{d_{p6}} = \frac{2*8.07}{2.362} = 6.833$lbf
The Pulley	$T_{Pulley}CCW = T_5 * \frac{N_G}{N_p} = 1.614 * \frac{60}{12} = 8.07$lbf-in	$F_P = \frac{2T_P}{d_{pp}} = \frac{2*8.07}{1} = 16.14$lbf

Motor force with 2 amp consideration: $0.33 * \frac{2}{2.45} = 0.269$lbf-in

7.2 - Belt Analysis Calculations

$$C_{P1} = \frac{1}{2}(\pi r) = \pi r = \pi(.275) = .8639\ in$$

$$C_{P2} = \frac{1}{2}(\pi r) = \pi r = \pi(.325) = 1.0210\ in$$

$$2C = L - C_{P1} - C_{P2} = 12 - .8639 - 1.0210 = 10.115$$

$$C = 5.0575\ in$$

$$\phi_{P1} = \pi - Sin^{-1}(\frac{D-d}{2}) = \pi - Sin^{-1}(\frac{.65-.55}{2}) = 3.122\ Rad$$

$$\phi_{P2} = \pi + Sin^{-1}(\frac{D-d}{2}) = \pi + Sin^{-1}(\frac{.65-.55}{2}) = 3.161\ Rad$$

$$F_C = \frac{w}{g}(\frac{V}{60})^2 = \frac{8.819x10^{-3}}{32.17}(\frac{113.752}{60})^2 = 9.85x10^{-4}lbf$$

$$E = \frac{FL}{A\Delta L} \rightarrow F_T = \frac{EA\Delta L}{L} = \frac{870.226(.02)(12.16)}{12} = 17.637\ lbf$$

$$\tau = (F_1 - F_2)r_1 \rightarrow (F_1 - F_2) = \frac{\tau}{r_1} \rightarrow (F_1 - F_2) = \frac{8.07}{.275} = 29.346\ lbf - in$$

$$F_1 = F_T + F_c + (\frac{F_1 - F_2}{2}) = 17.637 + 9.85x10^{-4} + (\frac{29.346}{2}) = 32.223\ lbf$$

$$F_2 = F_T + F_c - (\frac{F_1 - F_2}{2}) = 17.637 + 9.85x10^{-4} - (\frac{29.346}{2}) = 2.877\ lbf$$

$$\tau = (F_1 - F_2)r_2 \rightarrow (F_1 - F_2) = \frac{\tau}{r_2} \rightarrow (F_1 - F_2) = \frac{8.07}{.325} = 24.831\ lbf - in$$

$$F_1 = F_T + F_c + (\frac{F_1 - F_2}{2}) = 17.637 + 9.85x10^{-4} + (\frac{24.831}{2}) = 30.054\ lbf$$

$$F_2 = F_T + F_c - (\frac{F_1 - F_2}{2}) = 17.637 + 9.85x10^{-4} - (\frac{24.831}{2}) = 5.223\ lbf$$

7.3 - Reaction Forces and Moments, Inertia, and Deflections of Shafts

Shaft	$R_1 = R_2 = \frac{F}{2}$	$M_1 = M_2 = \frac{FL}{8}$	$I = \frac{\pi d^4}{64}$
A	$\frac{F_1}{2} = 0.570\ lbf$	$\frac{F_1 L_1}{8} = 0.185\ lbf * in$	$\frac{\pi {d_A}^4}{64} = 3.217 * 10^{-5}\ in^4$
B	$\frac{F_2}{2} = 0.569\ lbf$	$\frac{F_2 L_2}{8} = 0.142\ lbf * in$	$\frac{\pi {d_B}^4}{64} = 7.854 * 10^{-5}\ in^4$
C	$\frac{F_3}{2} = 1.140\ lbf$	$\frac{F_3 L_3}{8} = 0.285\ lbf * in$	$\frac{\pi {d_C}^4}{64} = 7.854 * 10^{-5}\ in^4$
E	$\frac{F_5}{2} = 3.419\ lbf$	$\frac{F_5 L_5}{8} = 0.855\ lbf * in$	$\frac{\pi {d_E}^4}{64} = 4.533 * 10^{-4}\ in^4$
F	$\frac{F_6}{2} = 3.417\ lbf$	$\frac{F_6 L_6}{8} = 0.854\ lbf * in$	$\frac{\pi {d_F}^4}{64} = 4.533 * 10^{-4}\ in^4$
G	$\frac{F_P}{2} = 8.070\ lbf$	$\frac{F_P L_P}{8} = 2.018\ lbf * in$	$\frac{\pi {d_G}^4}{64} = 4.533 * 10^{-4}\ in^4$

7.4 - Factor of Safety for gear train shafts based on our chosen Fatigue Failure Criteria

Shaft 1 - $\tau_m = 46.155\ Psi$ $\tau_a = 46.155\ Psi$

Goodman - $n_f = (\frac{\tau_a}{S_e} + \frac{\tau_m}{S_{ut}})^{-1} = (\frac{46.155}{800.68} + \frac{46.155}{10000})^{-1} = 16.06$

SWT (Smith-Watson-Topper) - $n_f = \frac{S_e}{\sqrt{(\tau_m+\tau_a)\tau_a}} = \frac{800.68}{\sqrt{(46.155+46.155)46.155}} = 12.27$

Shaft 2 - $\tau_m = 149.04\ Psi \quad \tau_a = 149.04\ Psi$

Goodman - $n_f = (\frac{\tau_a}{S_e} + \frac{\tau_m}{S_{ut}})^{-1} = (\frac{149.04}{800.68} + \frac{149.04}{10000})^{-1} = 4.97$

SWT (Smith-Watson-Topper) - $n_f = \frac{S_e}{\sqrt{(\tau_m+\tau_a)\tau_a}} = \frac{800.68}{\sqrt{(149.04+149.04)149.04}} = 3.80$

Shaft 3 - $\tau_m = 158.115\ Psi \quad \tau_a = 158.115\ Psi$

Goodman - $n_f = (\frac{\tau_a}{S_e} + \frac{\tau_m}{S_{ut}})^{-1} = (\frac{158.115}{800.68} + \frac{158.115}{10000})^{-1} = 4.69$

SWT (Smith-Watson-Topper) - $n_f = \frac{S_e}{\sqrt{(\tau_m+\tau_a)\tau_a}} = \frac{800.68}{\sqrt{(158.115+158.115)158.115}} = 3.58$

Shaft 4 - $\tau_m = 424.02\ Psi \quad \tau_a = 424.02\ Psi$

Goodman - $n_f = (\frac{\tau_a}{S_e} + \frac{\tau_m}{S_{ut}})^{-1} = (\frac{424.02}{800.68} + \frac{424.02}{10000})^{-1} = 1.75$

SWT (Smith-Watson-Topper) - $n_f = \frac{S_e}{\sqrt{(\tau_m+\tau_a)\tau_a}} = \frac{800.68}{\sqrt{(424.02+424.02)424.02}} = 1.34$

7.5 - Statistical analysis and FBD of Scissor Lifts Top Plate and Arms Under Static Load

$$k_a = stiffness\ of\ shaft\ A, k_b = stiffness\ of\ shaft\ B, k_C = Stiffness\ of\ Shaft\ C,$$

$$k_D = stiffness\ of\ shaft\ D, k_E = stiffness\ of\ shaft\ E$$

$$\underline{k_A = 0.322lb/in, k_B = k_C = 0.357lb/in, k_D = k_E = 2.063lb/in}$$

$$\frac{V_{top\ plate} * \rho_{top\ plate}}{l} = .286lb/in$$

Angles between arms and horizontal surfaces discovered via: $cos^{-1}(\frac{3.82}{7}) = 56.93$, the angle

between arms discovered via: $180 - 2(56.93) = 66.15$

Overall Length $l = 3.82 + 3.73 = 7.55$ in, distance between roller R_2 and the right end equals 3.73in, and the distance between the left end's R_1 and the R_2 is 3.73in.

Looking at the point load shown in Figure (Superposition 2):

Using Table A9, 10 where $l = 7.55, a = 3.82, b = 3.73$

Reaction forces for the left pin are $F_y{}' = \frac{fb}{l} = \frac{5(3.73)}{7.55} = 2.47$lbf and $F_x = 0$

Reaction forces for the roller is $F_{y2}{}' = \frac{fa}{l} = \frac{5(3.82)}{7.55} = 2.53$lbf

Forces from distributed .286lb/in load:

Looking at Table A9,7 where $w = .286, l = 3.82$

Reaction force $F_{y_1}{}'' = F_{y_2}{}' = \frac{wl}{2} = \frac{.286*3.82}{2} = 0.546lb$

Total forces

$$F_{y_1} = F_{y_1}{}' + F_{y_1}{}'' = 2.47 + 0.546 = 3.016lbf$$

$$F_{y_2} = F_{y_2}{}' + F_{y_2}{}'' = 2.53 + 0.546 = 3.076\text{lbf}$$

$$\theta = cos^{-1}(\frac{3.82}{7}) = 56.93 \text{ degrees}$$

$$\sum \quad M_B = 0 = F_{y1}2Lcos(\theta) - P_yLcos(\theta) - P_xLsin(\theta)$$

$$0 = -F_{y1} + P_y + R_{y1}$$

$$\sum \quad M_A = 0 = -F_{y2}2Lcos(\theta) - P_yLcos(\theta) + P_xLsin(\theta)$$

$$0 = -F_{y2} - P_y + R_{y2}$$

$$P_y = \frac{F_{y1}2Lcos\theta - P_xLsin\theta}{Lcos\theta} = 2F_{y1} - P_xtan\theta$$

$$P_x = \frac{F_{y2}2Lcos\theta + P_yLcos\theta}{Lsin\theta} = \frac{1}{tan\theta}(2F_{y2} + P_y) = \frac{2F_{y2} + 2F_{y1}}{tan\theta} - P_x$$

$$2P_x = \frac{2(F_{y2} + F_{y1})}{tan\theta}$$

$$P_x = R_{x2} = \frac{F_{y2} + F_{y1}}{tan\theta} = \frac{3.076 + 3.016}{tan(56.93)} = 3.97lbf$$

$$P_y = 2F_{y1} - P_xtan\theta = 2F_{y1} - (\frac{2F_{y2}}{tan\theta} + \frac{P_y}{tan\theta})tan\theta$$

$$P_y = 2F_{y1} - 2F_{y2} - P_y$$

$$P_y = F_{y1} - F_{y2} = 3.016 - 3.076 = -0.06lbf$$

$$0 = -F_{y1} + P_y + R_{y1}$$

$$R_{y1} = F_{y1} - P_y = 3.016 - (-0.06) = 3.076lbf$$

$$0 = -F_{y2} - P_y + R_{y2}$$

$$R_{y2} = F_{y2} + P_y = 3.076 - 0.06 = 3.016lbf$$

Summarized results from Free Body Diagram:

$$P_x = R_{x2} = 3.97lbf$$

$$P_y = -0.06lbf$$

$$R_{y1} = 3.076lbf$$

$$R_{y2} = 3.016lbf$$

Table A9: 14 (for the beams)

7.6 - The stiffnesses for each member in the joint for each selected bolts

Youngs Modulus: $E_{Al} = 10.3 * 10^6$ psi $E_{Steel} = 30 * 10^6$ psi

7.6.1 - Stiffness Calculations for Material Under Load

$$K_{plate} = \frac{.5774 * E_{Aluminum} * \pi * .164}{ln\left(\frac{(1.155t + D - d)(D + d)}{(1.155t + D - d)(D + d)}\right)} = \frac{.5774 * 10.3 * 10^6 * \pi * .164}{ln\left(\frac{((1.155 * \frac{1}{8}) + .540 - .164)(.563 + .164)}{((1.155 * \frac{1}{8}) + .540 + .164)(.563 - .164)}\right)}$$

$$= 2528125.239\frac{lbf}{in}$$

$$K_{washer} = \frac{.5774\pi E}{2 * ln\left(5 * \frac{(.5774 * l) + (.5d)}{(.5774 * l) + (2.5d)}\right)} = \frac{.5774 * \pi * 30 * 10^6}{2 * ln\left(5 * \frac{(.5774 * .03) + (.5 * .164)}{(.5774 * .03) + (2.5 * .164)}\right)}$$

$$= 181073029.6\frac{lbf}{in}$$

$$K_m = \left(\frac{2}{K_{plate}} + \frac{2}{K_{washer}}\right)^{-1} = \left(\frac{2}{2528125.239} + \frac{2}{181073029.6}\right)^{-1} = 10594150.69\frac{lbf}{in}$$

$$l_t = \frac{1}{2}in$$

$A_t = .01474in^2$ from table 8-2

$$K_b = \frac{A_t A_d E_{Steel}}{A_d l_t + A_t l_d} \quad \text{since } l_d = 0,\ K_b = \frac{A_t E_{Steel}}{l_t} = \frac{.01474*30*10^6}{.5} = 884400$$

7.6.2 - Stiffness Calculations for Load on Top Plate of Scissor Lift

$$E_{pvc} = 3275\ MPa \rightarrow 474998.6\ Psi\ [4]$$

$$K_{plate} = \frac{.5774 * E_{Aluminum} * \pi * .164}{ln\left(\frac{(1.155t + D - d)(D + d)}{(1.155t + D - d)(D + d)}\right)} = \frac{.5774 * 10.3 * 10^6 * \pi * .164}{ln\left(\frac{((1.155 * \frac{1}{8}) + .540 - .164)(.563 + .164)}{((1.155 * \frac{1}{8}) + .540 + .164)(.563 - .164)}\right)}$$

$$= 2528125.239 \frac{lbf}{in}$$

$$K_{washer} = \frac{.5774\pi E}{2 * ln\left(5 * \frac{(.5774 * l) + (.5d)}{(.5774 * l) + (2.5d)}\right)} = \frac{.5774 * \pi * 30 * 10^6}{2 * ln\left(5 * \frac{(.5774 * .03) + (.5 * .164)}{(.5774 * .03) + (2.5 * .164)}\right)}$$

$$= 181073029.6 \frac{lbf}{in}$$

$$K_{pvc} = \frac{.5774 * E_{PVC} * \pi * .164}{ln\left(\frac{(1.155t + D - d)(D + d)}{(1.155t + D - d)(D + d)}\right)} = \frac{.5774 * 474998.6 * \pi * .164}{ln\left(\frac{((1.155 * .125) + .540 - .164)(.563 + .164)}{((1.155 * .125) + .540 + .164)(.563 - .164)}\right)}$$

$$= 1106618.768 \frac{lbf}{in}$$

$$K_m = \left(\frac{2}{K_{plate}} + \frac{2}{K_{washer}} + \frac{1}{K_{pvc}}\right)^{-1} = \left(\frac{2}{2528125.239} + \frac{2}{181073029.6} + \frac{1}{110618.768}\right)^{-1}$$

$$= 1001958.548 \frac{lbf}{in}$$

$$l_t = \frac{1}{2} in$$

$$K_b = \frac{A_t A_d E_{Steel}}{A_d l_t + A_t l_d} \quad \text{since } l_d = 0,\ K_b = \frac{A_t E_{steel}}{l_t} = \frac{.01474*30*10^6}{.5} = 884400$$

7.6.3 - Stiffness Calculation for Dynamic Arm Movement

$$K_{plate} = \frac{.5774 * E_{Aluminum} * \pi * .164}{ln\left(\frac{(1.155t + D - d)(D + d)}{(1.155t + D - d)(D + d)}\right)} = \frac{.5774 * 10.3 * 10^6 * \pi * .164}{ln\left(\frac{((1.155 * \frac{1}{8}) + .540 - .164)(.563 + .164)}{((1.155 * \frac{1}{8}) + .540 + .164)(.563 - .164)}\right)}$$

$$= 2528125.239 \frac{lbf}{in}$$

$$K_{washer} = \frac{.5774\pi E}{2 * ln\left(5 * \frac{(.5774 * l) + (.5d)}{(.5774 * l) + (2.5d)}\right)} = \frac{.5774 * \pi * 30 * 10^6}{2 * ln\left(5 * \frac{(.5774 * .03) + (.5 * .164)}{(.5774 * .03) + (2.5 * .164)}\right)}$$

$$= 181073029.6 \frac{lbf}{in}$$

$$K_m = \left(\frac{2}{K_{plate}} + \frac{2}{K_{washer}}\right)^{-1} = \left(\frac{2}{2528125.239} + \frac{2}{181073029.6}\right)^{-1} = 10594150.69 \frac{lbf}{in}$$

$$l_t = \frac{3}{4} in$$

$K_b = \frac{A_t A_d E_{Steel}}{A_d l_t + A_t l_d}$ since $l_d = 0$, $K_b = \frac{A_t E_{Steel}}{l_t} = \frac{.01474 * 30 * 10^6}{.75} = 589600$

7.7 - Stiffness Constant and Load Taken on by each Bolts

For Figure 13 and 14

$$C = \frac{k_b}{k_b + k_m} = \frac{884400}{884400 + 10594150.69} = .077$$

For Figure 15 and 16

$$C = \frac{k_b}{k_b + k_m} = \frac{884400}{884400 + 1001958.548} = .4688$$

For Figure 17 and 18

$$C = \frac{k_b}{k_b + k_m} = \frac{589600}{589600 + 10594150.69} = .37$$

7.8 - Torque load on each selected bolt

S_y from [5]

$$S_P = 0.85 S_y = 0.85(205 * 10^6) = 174.25\ MPa = \ 25.273\ kpsi$$

Nonpermanent Fasteners, thus 75% Proof Load: $F_i = 0.75 A_t S_p$

$$F_i = 0.75 A_t S_p = 0.75(.01474)(25.273 * 10^3) = 279.39 lb$$

Machine screw: K = 0.3 (nonplated)

$$\tau = K F_i d = 13.75 bl - in$$

All 3 iterations of the bolt would be under the same estimated torque.

7.9 - Tensile Stress and the Factor of Safety For Static Stress on each Bolt

Only one bolt selected doesn't have members in tension

$$R_{y2} = 3.016\ lbf = P, \sigma_{b1} = \frac{0.077(3.016)+279.39}{0.01474} = 18.97\ kpsi, n_{p1} = \frac{25.273}{18.97} = 1.33$$

$$W = 0.0914lb, \sigma_{b3} = \frac{0.37(0.0914) + 279.39}{0.01474} = 18.96\ kpsi, n_{p3} = \frac{25.273}{18.96} = 1.33$$

7.10 - Factor of Safety the situations of overloading and load separation on the selected bolt

Factor of Safety for Figure 13 & 14 -

$$n_L = \frac{S_p A_t - F_i}{CP} = \frac{(25.273 * 10^3)(.0174) - (279.39)}{(0.077)(3.016)} = 401.04$$

$$n_0 = \frac{F_i}{P(1-C)} = \frac{P_0}{P} = \frac{(279.39)}{(3.016)(1-0.077)} = 100.36$$

Factor of Safety for Figure 15 & 16 - Cant be obtained because the Bolt is not under Tension so Stress is Zero so our Factor of Safety is Zero.

Factor of Safety for Figure 17 and 18 -

$$n_L = \frac{S_p A_t - F_i}{CP} = \frac{(25.273 * 10^3)(0.01475) - (279.39)}{(0.37)(3.016)} = 83.46$$

$$n_0 = \frac{F_i}{P(1-C)} = \frac{P_0}{P} = \frac{(279.39)}{(3.016)(1-0.37)} = 147.04$$

7.11 - Calculate the Minimum and Maximum load on the selected bolts

For Figure 13 and 14

$$F_{bmin} = CP_{min} + F_i = .077 * 0 + 279.39 = 279.3lb$$

$$F_{max} = CP_{max} + F_i = .077 * 3.016 + 279.39 = 279.622lb$$

For Figure 15 and 16

$$F_{bmin} = CP_{min} + F_i = .4688 * 0 + 279.39 = 279.3lb$$

$$F_{max} = CP_{max} + F_i = .4688 * 3.016 + 279.39 = 280.803lb$$

For Figure 17 and 18

$$F_{bmin} = CP_{min} + F_i = .37 * 0 + 279.39 = 279.3lb$$

$$F_{max} = CP_{max} + F_i = .37 * 3.016 + 279.39 = 280.505lb$$

7.12 - Moments of Walls and Max Force from bearing

$$M = (.02)(8.07)(\frac{.31}{2}) = .025\ lb * in$$

$$F = \frac{.025}{.9} = .0278\ lb$$

7.13 - Gear Train Shaft Tolerances

For the smallest transmission (0.16 inches):
According to Table 13- $\Delta D = 0.0007$ in and $\Delta d = 0.0005$ in
According to Table 14- $\delta_F = -0.0004$ in
$D = d = D_{min} = 0.16$ in
$D_{max} = D + \Delta D = 0.16 + 0.0007 = 0.1607$ in
$d_{max} = d + \delta_F = 0.16 + (-0.0004) = 0.1596$ in
$d_{min} = d + \delta_F - \Delta d = 0.16 + (-0.0004) - 0.0005 = 0.1591$ in

For the other small transmission (0.2 inches):
According to Table 13- $\Delta D = 0.0007$ in and $\Delta d = 0.0005$ in
According to Table 14- $\delta_F = -0.0004$ in
$D = d = D_{min} = 0.2$ in
$D_{max} = D + \Delta D = 0.2 + 0.0007 = 0.2007$ in
$d_{max} = d + \delta_F = 0.2 + (-0.0004) = 0.1996$ in
$d_{min} = d + \delta_F - \Delta d = 0.2 + (-0.0004) - 0.0005 = 0.1991$ in

For the larger transmission (0.31 inches):
According to Table 13- $\Delta D = 0.0009$ in and $\Delta d = 0.0006$ in
According to Table 14- $\delta_F = -0.0005$
$D = d = D_{min} = 0.31$ in
$D_{max} = D + \Delta D = 0.31 + 0.0009 = 0.3109$ in
$d_{max} = d + \delta_F = 0.31 + (-0.0005) = 0.3095$ in
$d_{min} = d + \delta_F - \Delta d = 0.31 + (-0.0005) - 0.0006 = 0.3089$ in

For the Diameter of the holes and shafts in the brackets (0.24 inches):
According to Table 13- $\Delta D = 0.0009$ in and $\Delta d = 0.0006$ in
According to Table 14- $\delta_F = -0.0005$
$D = d = D_{min} = 0.24$ in
$D_{max} = D + \Delta D = 0.24 + 0.0009 = 0.2409$ in
$d_{max} = d + \delta_F = 0.24 + (-0.0005) = 0.2395$ in
$d_{min} = d + \delta_F - \Delta d = 0.24 + (-0.0005) - 0.0006 = 0.2389$ in

7.14 - Stress Concentration Calculations

12-24T shaft: (r/d) = (0.0394/0.1575) = 0.25, (d/D) = 1.25,

K = 1.19

12-36T shaft: (r/d) = (0.0787/0.1575) = 0.5, (D/d) = 1.5, K = 1.19, 1

12-60T Shaft: K = 1.19

7.15 - Belt Force Analysis

$$C_{P1} = \frac{1}{2}(\pi r) = \pi r = \pi(.275) = .8639\ in$$

$$C_{P2} = \frac{1}{2}(\pi r) = \pi r = \pi(.325) = 1.0210\ in$$

$$2C = L - C_{P1} - C_{P2} = 12 - .8639 - 1.0210 = 10.115\ in$$

$$C = 5.0575\ in$$

Next we wanted to find the belt's angles of attachment to ensure we had enough surface area. (Figure 9)

$$\phi_{P1} = \pi - Sin^{-1}(\frac{D-d}{2}) = \pi - Sin^{-1}(\frac{.65-.55}{2}) = 3.122\ Rad$$

$$\phi_{P2} = \pi + Sin^{-1}(\frac{D-d}{2}) = \pi + Sin^{-1}(\frac{.65-.55}{2}) = 3.161\ Rad$$

$$F_C = \frac{w}{g}(\frac{V}{60})^2 = \frac{8.819x10^{-3}}{32.17}(\frac{113.752}{60})^2 = 9.85 * 10^{-4} lbf$$

$$E = \frac{FL}{A\Delta L} \rightarrow F_T = \frac{EA\Delta L}{L} = \frac{870.226(.02)(12.16)}{12} = 17.637\ lbf$$

Tension on each end of 1st Pulley (Figure 10)

$$\tau = (F_1 - F_2)r_1 \rightarrow (F_1 - F_2) = \frac{\tau}{r_1} \rightarrow (F_1 - F_2) = \frac{8.07}{.275} = 29.346\ lbf - in$$

$$F_1 = F_T + F_c + (\frac{F_1 - F_2}{2}) = 17.637 + 9.85 * 10^{-4} + (\frac{29.346}{2}) = 32.223\ lbf$$

$$F_2 = F_T + F_c - (\frac{F_1 - F_2}{2}) = 17.637 + 9.85 * 10^{-4} - (\frac{29.346}{2}) = 2.877\ lbf$$

Tension on each end of 2nd Pulley (Figure 11)

$$\tau = (F_1 - F_2)r_2 \rightarrow (F_1 - F_2) = \frac{\tau}{r_2} \rightarrow (F_1 - F_2) = \frac{8.07}{.325} = 24.831\ lbf - in$$

$$F_1 = F_T + F_c + (\frac{F_1 - F_2}{2}) = 17.637 + 9.85 * 10^{-4} + (\frac{24.831}{2}) = 30.054\ lbf$$

$$F_2 = F_T + F_c - (\frac{F_1 - F_2}{2}) = 17.637 + 9.85 * 10^{-4} - (\frac{24.831}{2}) = 5.223\ lbf$$